



DEVELOPMENT AND COMMISSIONING OF THE K500 SUPERCONDUCTING HEAVY ION CYCLOTRON

Sumit Som

**Variable Energy Cyclotron Centre
Department of Atomic Energy
Government of India
Kolkata, India**

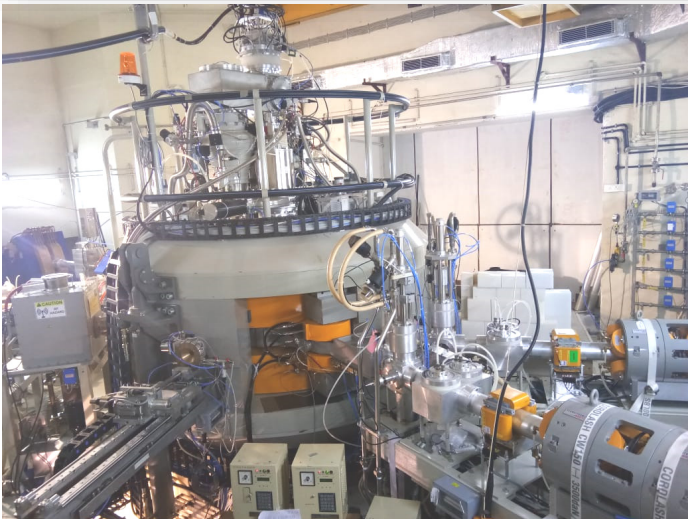
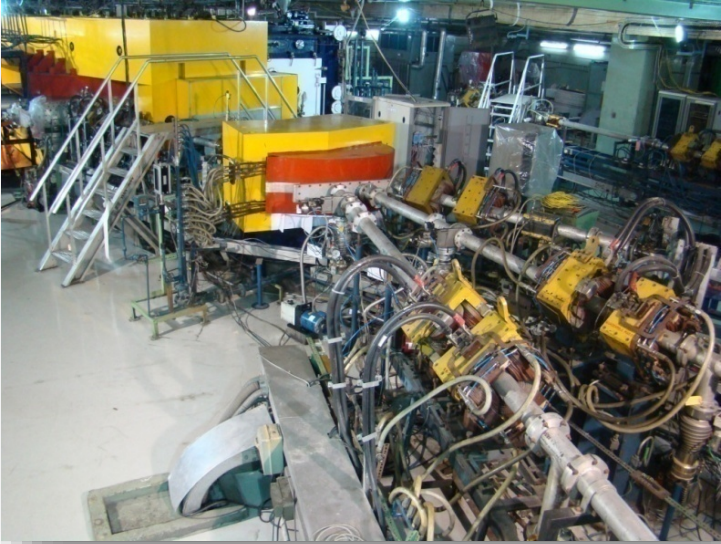
29 June 2022



VARIABLE ENERGY CYCLOTRON CENTRE KOLKATA, INDIA



OPERATING CYCLOTRONS: 3 NOS. (K130, CYCLONE30, K500)





Variable Energy Cyclotron Centre (VECC) is one of the R&D units under the **Department of Atomic Energy (DAE), Govt. Of India**. Primarily engaged in the area of **research in Basic Sciences** since its inception in 1969.

Major activities of VECC:

Basic Sciences:
Experimental Research in Low and High energy Nuclear Physics using accelerators and Theoretical Nuclear Physics

Accelerator based Applied Research in the field of material science & radiation damage studies

Societal applications : Medical Cyclotron for isotope production

Indigenous accelerator development and R&D on Advanced Accelerators

Technology Development:
RF/SRF Detectors DAQ Instrumentation
Power Electronics Mechanical Cryogenics Computer & IT services

Content

- 1. SC Cyclotron – a brief review**
- 2. Beam extraction trial**
- 3. Diagnosis of the beam extraction problem**
- 4. Magnetic Field Mapping and Correction**
- 5. Present Status**

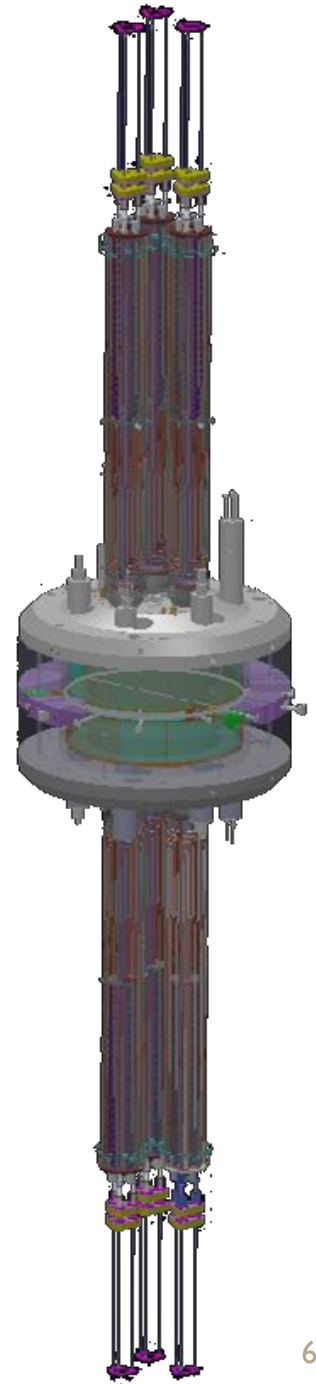
$K = 500$ SUPERCONDUCTING CYCLOTRON (SCC)

- **A pill-box type dipole magnet, energized by superconducting Nb-Ti coil operating at 4.2 K**
- **Magnetic field: 3 to 5 Tesla**
- **Very Compact, Accessibility restricted**
- **Flexible in terms of various ions and ion-energies**

First Superconducting Cyclotron: Michigan State University (1982)

The machine was replicated with minor modifications at TEXAS A&M University.

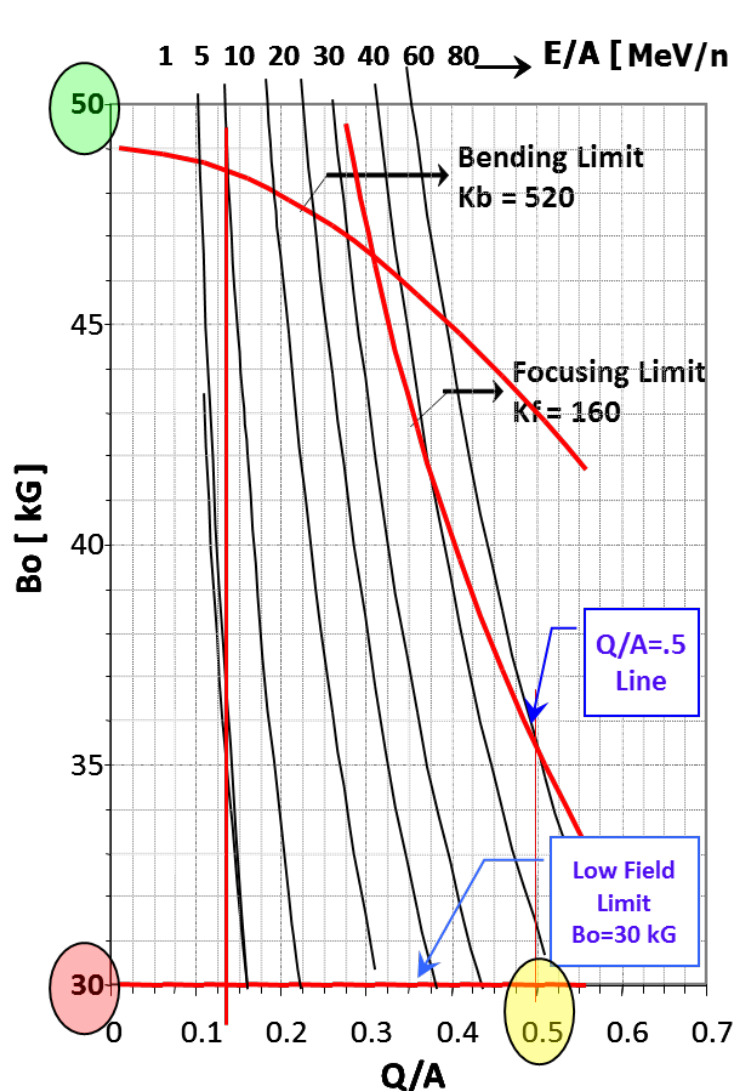
VECC SCC is based on TEXAS A&M K500 machine.



VECC K500 SUPERCONDUCTING CYCLOTRON



OPERATING REGION (IN CHARGE STATE-MAGNETIC FIELD PLANE)



$$K_b = \frac{e^2 B^2 R^2}{2m_p}$$

Lighter heavy ions: 80 MeV/u
Very heavy ions: 5-15 MeV/u

Low field limit at $B_0=30$ kG,
 due to $\nu_r + 2\nu_z = 3$ resonance

For $Q/A > 0.5$ the coupling resonance
 $\nu_r + 2\nu_z = 3$ resonance is encountered at
 internal radius

Medium and Heavier mass ions: The Energy is limited to

$$E/A \sim K_b (Q/A)^2 \text{ MeV/A, } K_b \sim 500$$

For Lighter Ions ($Q/A > 0.312$), The Energy is limited to

$$E/A \sim K_f (Q/A) \text{ MeV/A, } K_f \sim 160$$

MAGNET IRON STRUCTURE: (~ 80 TONNES)

- Upper and lower pole and return yoke
- Pole radius = 0.654 meter, three spiral hills, each covering an angle of 46° at the outer radii.
- Pole gap at hills = 64 mm.

- The poles having hill-valley sectors are installed on two end-plates
- The cylindrical iron return yoke extends from 1.066 meter radius to 1.524 meter radius.
- Median plane reflection symmetry



FABRICATION OF MAGNET IRON

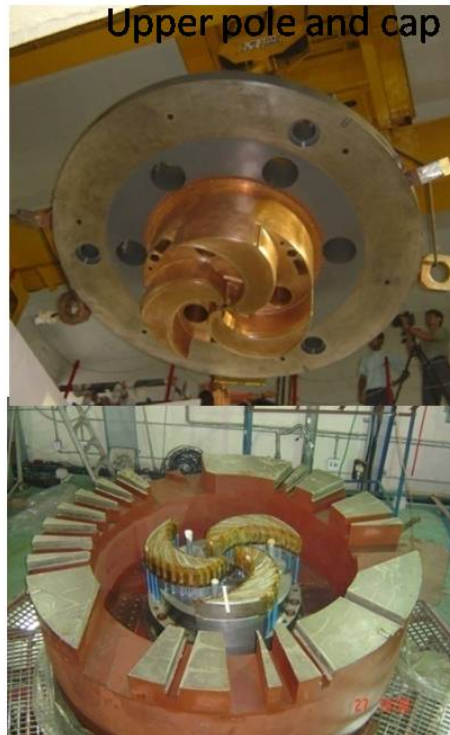
(done at M/s Heavy Engineering Corp., Ranchi, India)



Spiral Pole tips

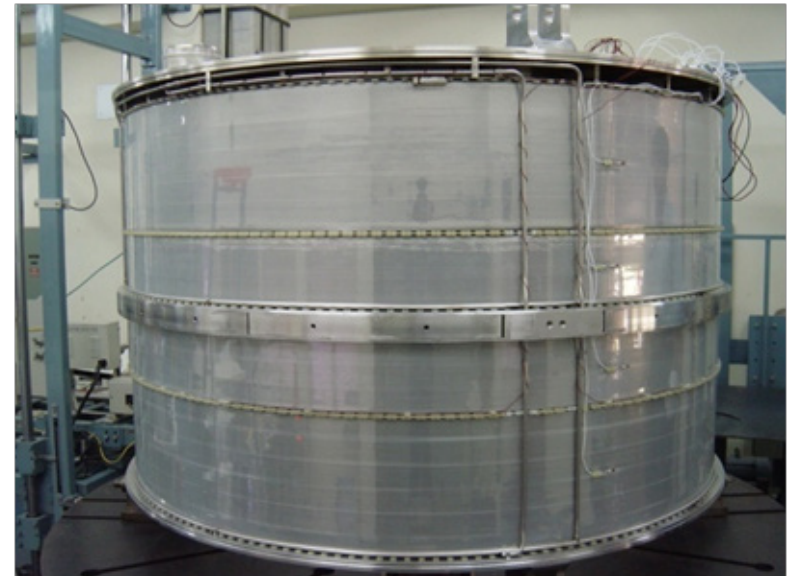


Pole base & Return Yoke



SUPERCONDUCTING COIL AND CRYOSTAT:

- Annular Cryostat between the pole and the return yoke (0.654 meter radius to 1.066 meter radius) houses the superconducting coils
- The coils are made of NbTi multifilament composite superconducting cable (with critical current 1030 A at 5.5 Tesla and 4.2 K), consisting of 500 filaments of 40 micron diameter embedded in copper matrix (1:20).
- There are two independently powered coils, namely the α coil and the β coil.

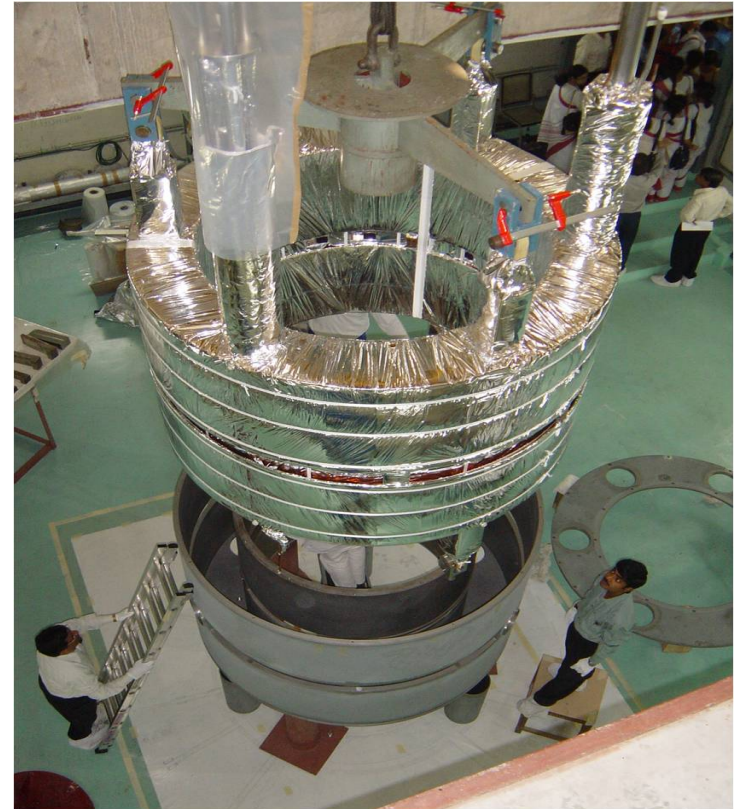


- The liquid helium chamber is wrapped with several layers of **multi-layer insulation (MLI)** sheets and outside it there is **liquid nitrogen (LN)** cooled thermal shield made of copper sheet. There are several layers of MLI wrappings outside the LN-shield also.
- The entire coil assembly (the liquid helium chamber and the Cu thermal shield wrapped with MLI layers) is then inserted into the cryostat vacuum chamber (coil-tank) made of magnetic steel
- The bobbin is kept suspended inside the coil-tank with the help of nine glass-epoxy support-links.
- There are **20 radial penetrations** welded on the outer surface of coil-tank at the median plane, used for inserting the drives for electrostatic deflectors and magnetic channels, beam diagnostic elements etc.
- **Cryogenic lines and the power feed-throughs** are connected from the top.





The upper half of magnet iron structure



The superconducting coil and liquid nitrogen cooled thermal shield, together wrapped in multilayer insulations, being inserted in the cryostat vacuum chamber (coil-tank)

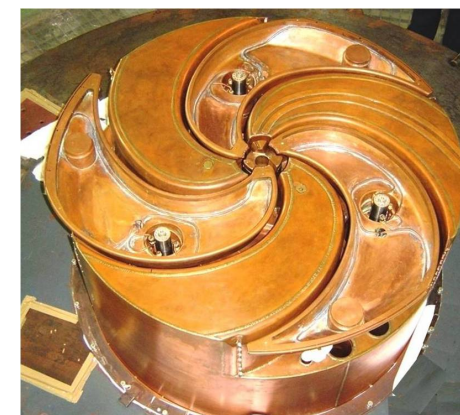
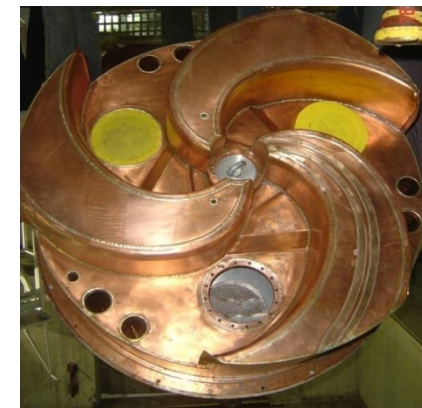
TRIM COILS

- There are **13 trim-coils** wound around each spiral pole-tips, below and above median plane. All these **78 trim coils are made of water-cooled copper conductor.**



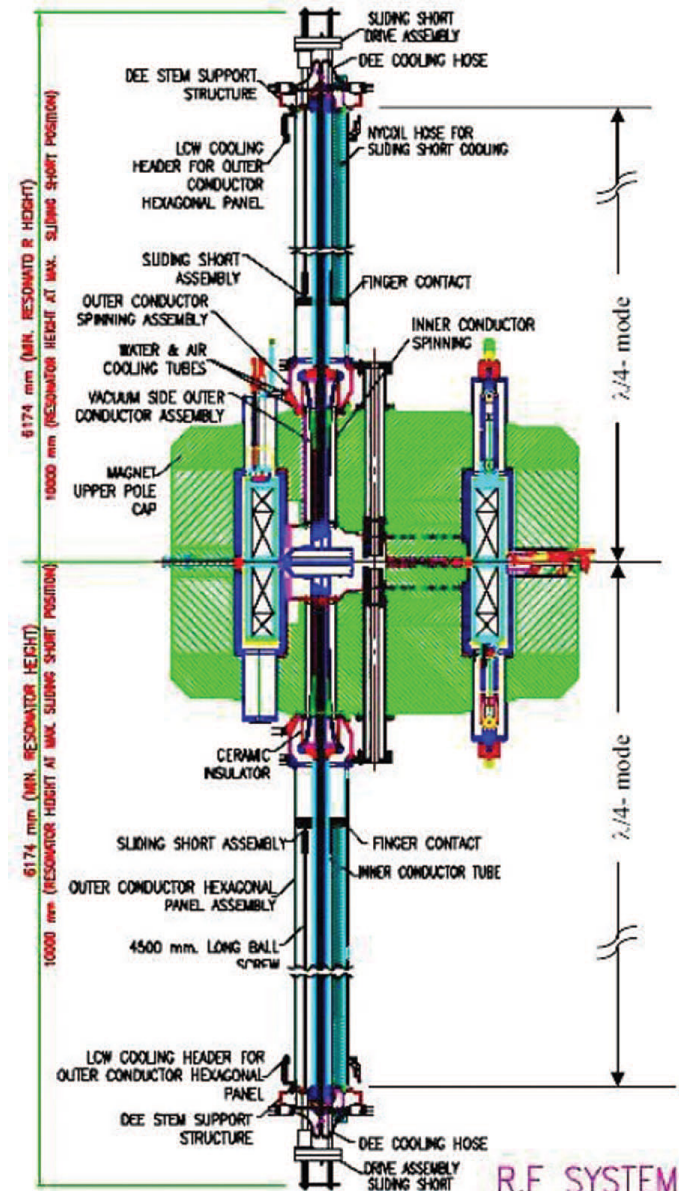
RADIO-FREQUENCY SYSTEM AND DEES:

- It comprises of three half-wave co-axial cavities made of copper, placed axially (vertically) with an angular distance of 120° between them.
- In this structure, the dees and the dee stems act as the inner conductor and the liner on the pole and the hexagonal panels as the outer conductor.
- **Three spiral Dees, each of 60° azimuthal width, situated in the three spiral valley regions.**
- Dees constitute the accelerating structures of the cyclotron.

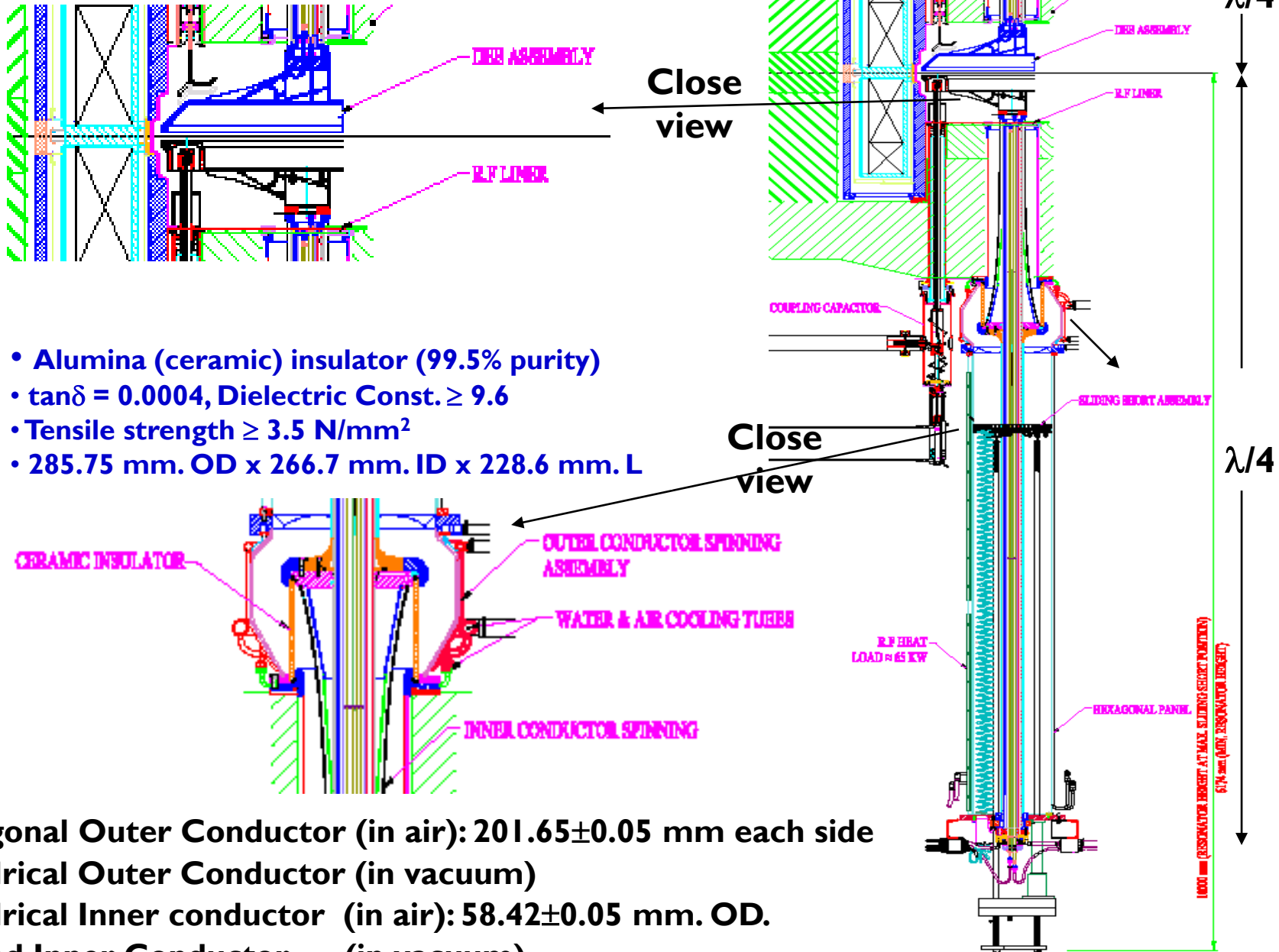


RADIO-FREQUENCY SYSTEM AND DEES:

- The **half-wave cavities** are actually combinations of two quarter wave cavities, one coming from the top and the other from the bottom
- The RF system is designed for a maximum dee voltage of around 80 kV and for a frequency range from **9 to 27 MHz** that is achieved by moving a sliding short provided in each of the six quarter wave cavities.
- The total RF structure extends 6m above and 6m below the cyclotron median plane.



MAIN DEE CAVITY WITH DEE STEM



- Alumina (ceramic) insulator (99.5% purity)
- $\tan\delta = 0.0004$, Dielectric Const. ≥ 9.6
- Tensile strength $\geq 3.5 \text{ N/mm}^2$
- 285.75 mm. OD x 266.7 mm. ID x 228.6 mm. L

- Hexagonal Outer Conductor (in air): $201.65 \pm 0.05 \text{ mm}$ each side
- Cylindrical Outer Conductor (in vacuum)
- Cylindrical Inner conductor (in air): $58.42 \pm 0.05 \text{ mm. OD.}$
- Tapered Inner Conductor (in vacuum)

FINAL RF AMPLIFIERS (3 X 80 KW) FOR K500 SCC



RF Amplifier feeding power to the cavity through Coupling Capacitor

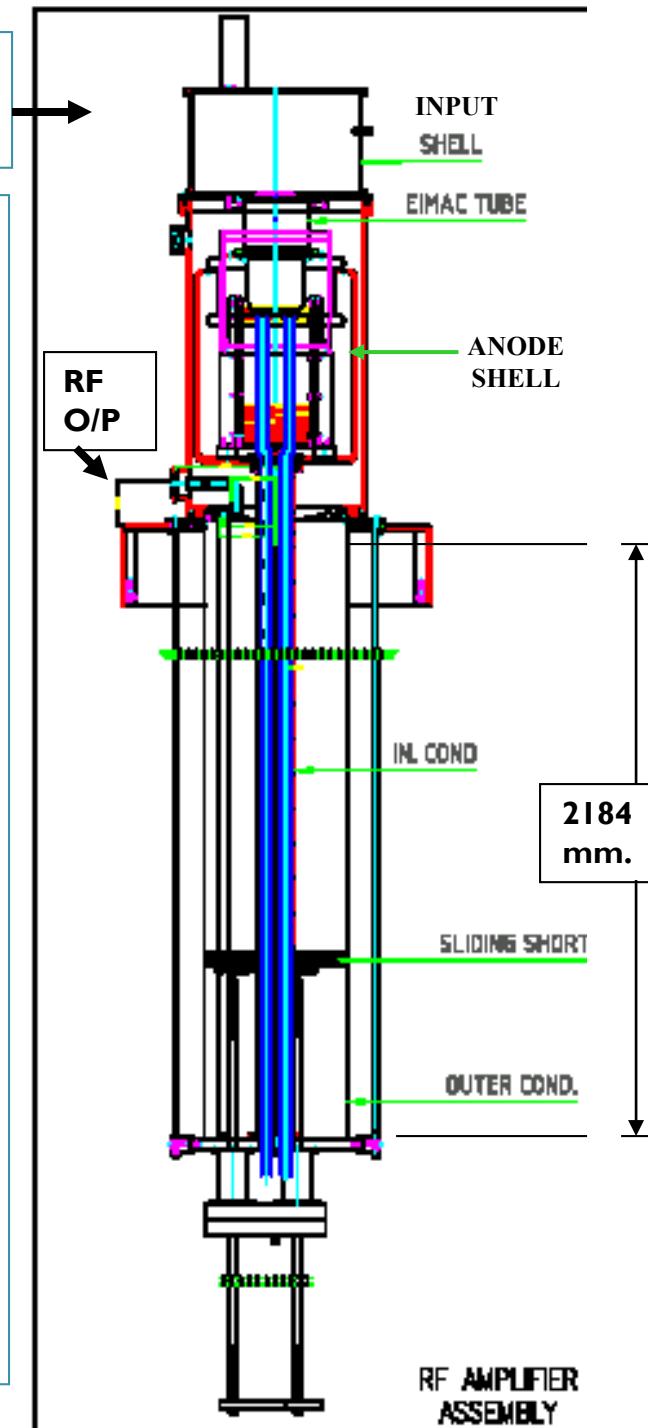
**RF AMPLIFIER
 TESTED with 50 Ω
 dummy load up to
 80 Kw at 27 MHz**

RF Amplifiers fabricated at VECC

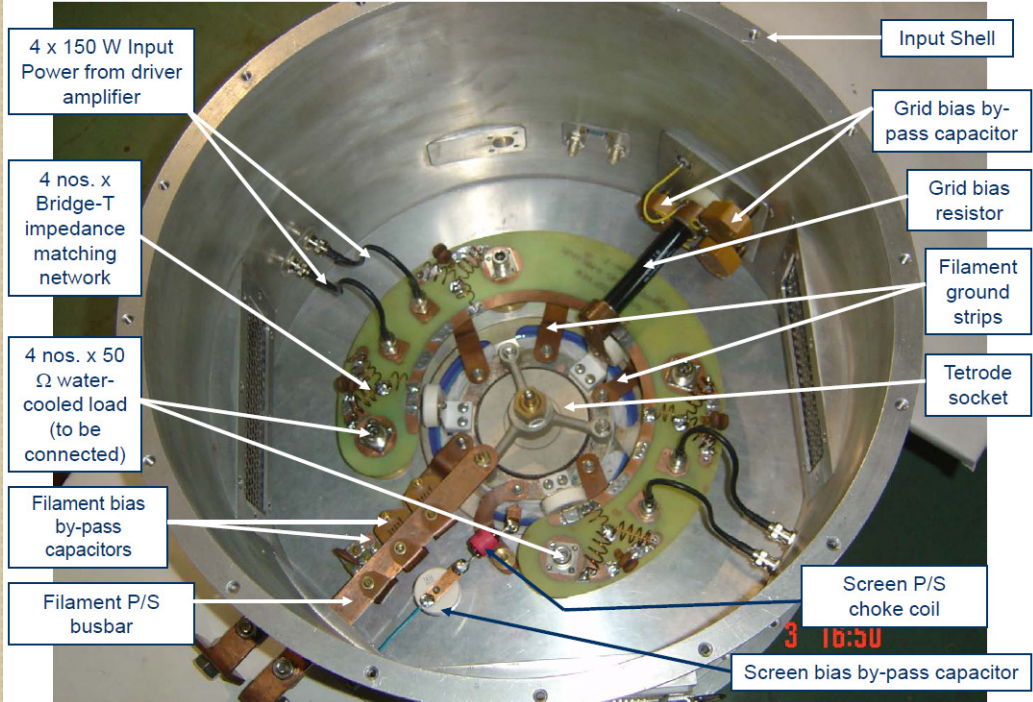


CROSS-SECTIONAL VIEW OF RF POWER AMPLIFIER

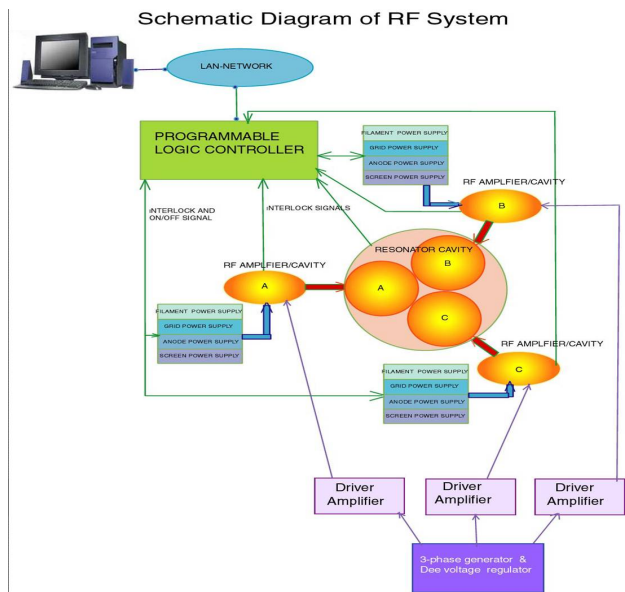
- Eimac 4CW 150000E Tetrode based power amplifier
- Output Power: 100 kW max. at 50 Ohm
- Power gain ~ 22 dB
- Input Power: 1kW at 50 Ohm
- Mode of operation: Class AB
- $\lambda/4$ Resonant cavity similar to main Dee-cavity
- Tunable from 9 MHz to 27 MHz by movable Sliding short
- Sliding short travel ~ 2184 mm. max.
- Precise movement of sliding short (with resolution ~ 50 $\mu\text{m}.$)



INPUT CIRCUIT FOR HIGH POWER RF AMPLIFIER



PLC-BASED INTERLOCKS FOR RF SYSTEM



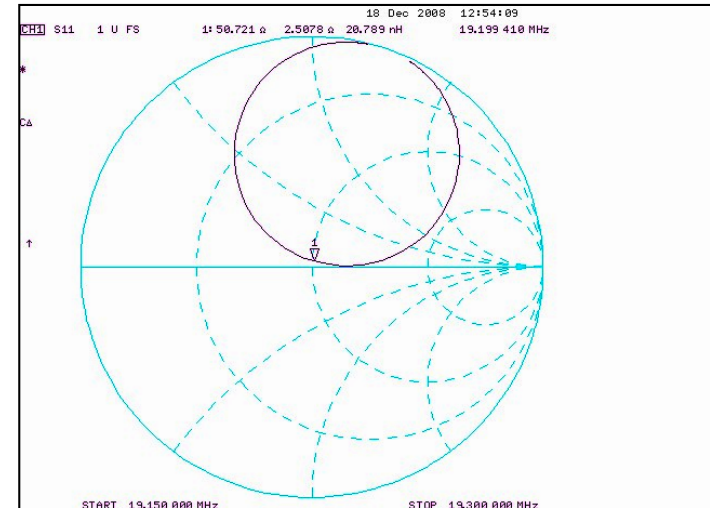
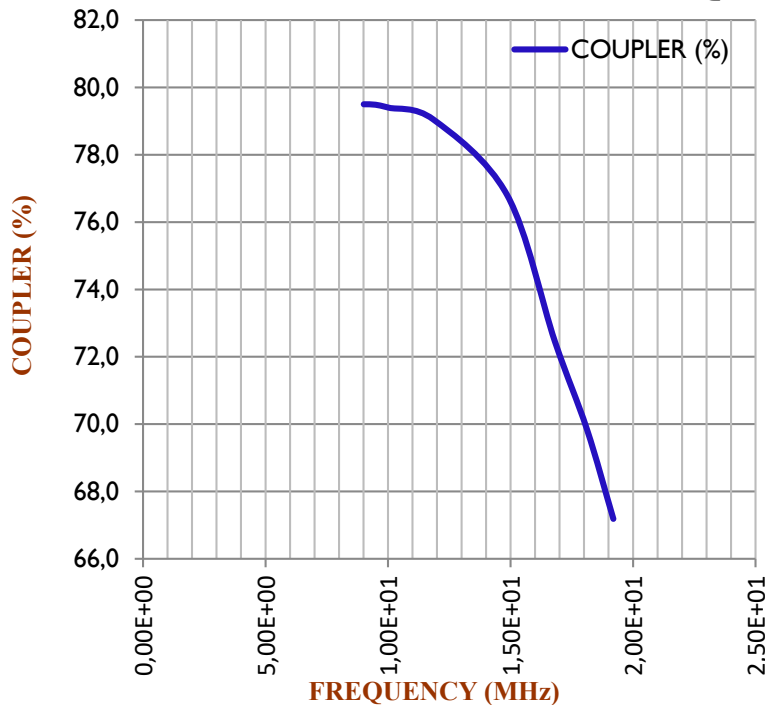
CAVITY IMPEDANCE MATCHING VIA COUPLER / TRIMMER / SLIDING SHORT

- Cavity shunt impedance matching to 50 Ω == Sliding Short Position, Trimmer Pos. Coupler Pos.,
- Very sensitive
- S_{11} measurement
- $Z = 50.721 + j2.507 \Omega$ at 19.1994 MHz

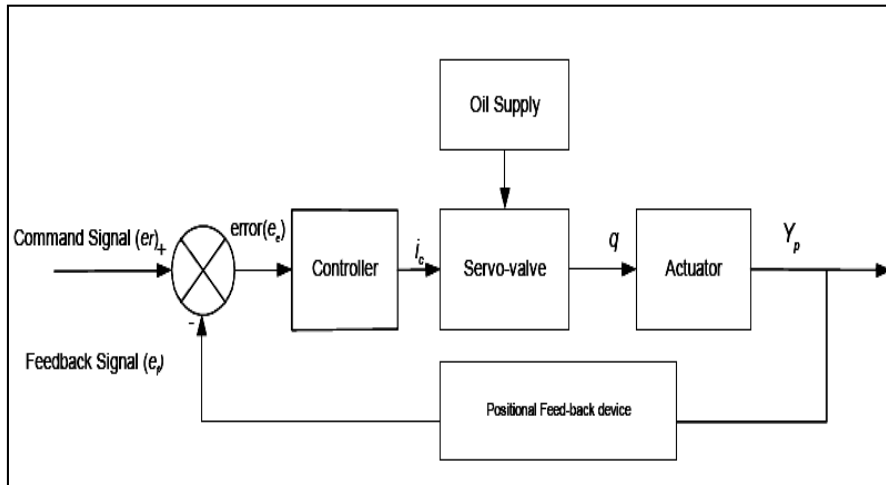
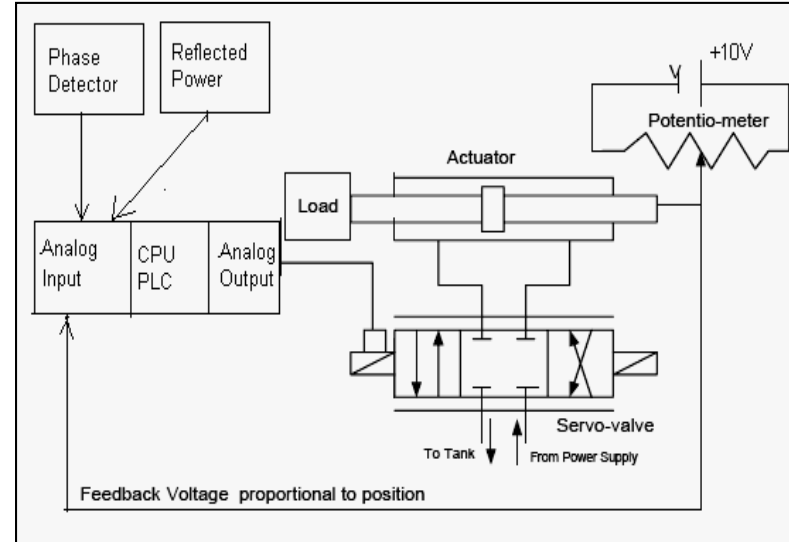
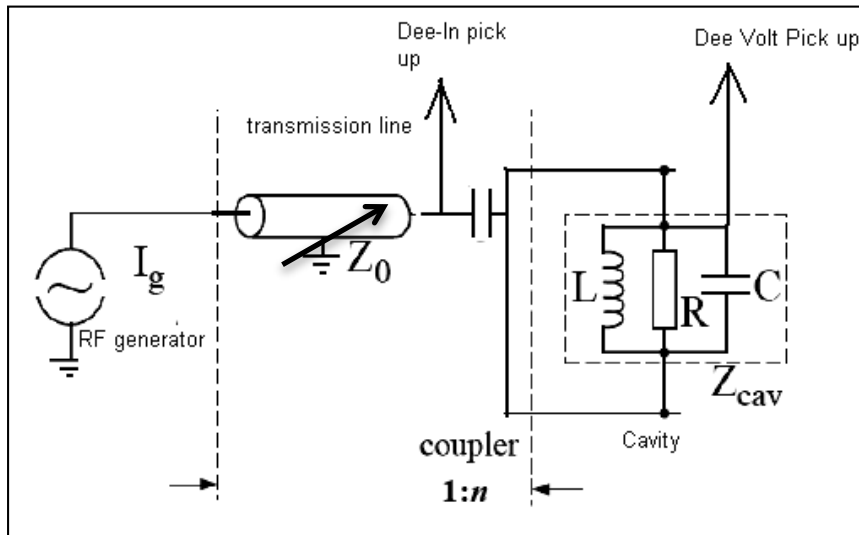


RF Power feeding to main cavity via Coupler

COUPLER Pos. vs. FREQUENCY



CLOSED-LOOP TRIMMER CONTROL

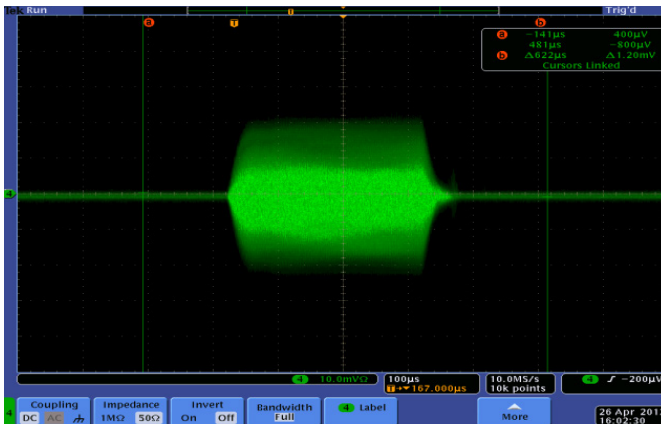
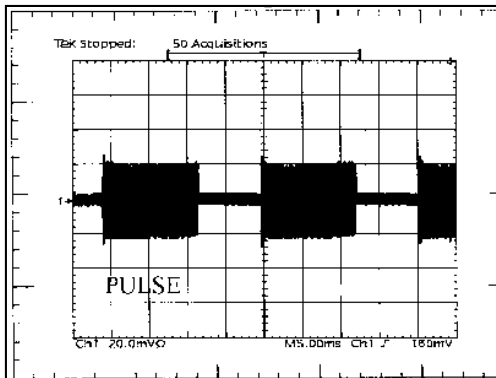


- Hydraulically driven trimmer movement with $20 \mu\text{m}$ accuracy
- indigenous development of coupler & closed-loop trimmer control system

Published:

“Closed Loop rf tuning for superconducting Cyclotron at VECC” by A. Mandal, S. Som, et. al., Proceedings in the International Conference on Cyclotrons and their Applications (CYCLOTRONS-2010), China

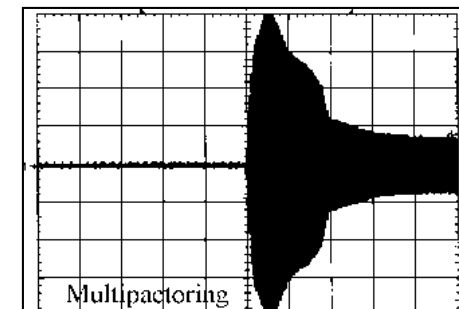
MEASUREMENT OF CAVITY QUALITY FACTOR WITH POWER (PULSED) (BY MEASURING CAVITY TIME CONSTANT, τ)



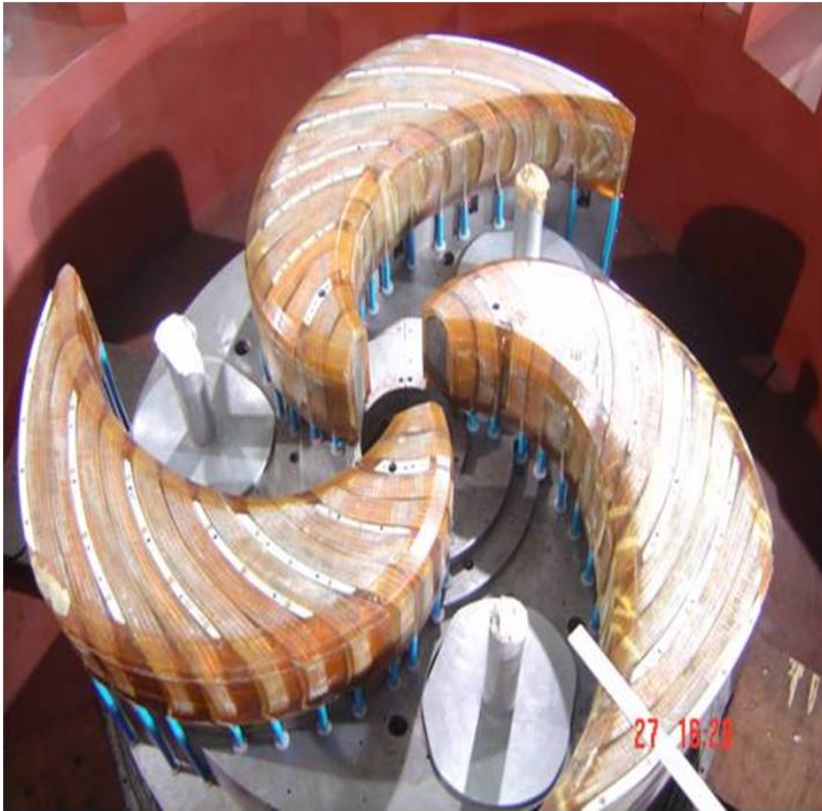
- Pulsing the cavity with 14 MHz RF
- Pulse ON time: 300 μ S
- Pulse duty cycle: 10%
- Cavity time constant, $\tau=39.8 \mu$ S (Measured)
- $\tau=2Q_L/\omega_0$ [$f_0=14$ MHz]
- $Q_L = 1750$
- $Q_0=2Q_L=3500$ (critically coupled)
- $\tau=21.6 \mu$ S (Measured)
- $Q_L = 1425$ & $Q_0=2840$ [$f_0=21$ MHz].

3D CST MWS Simulation:

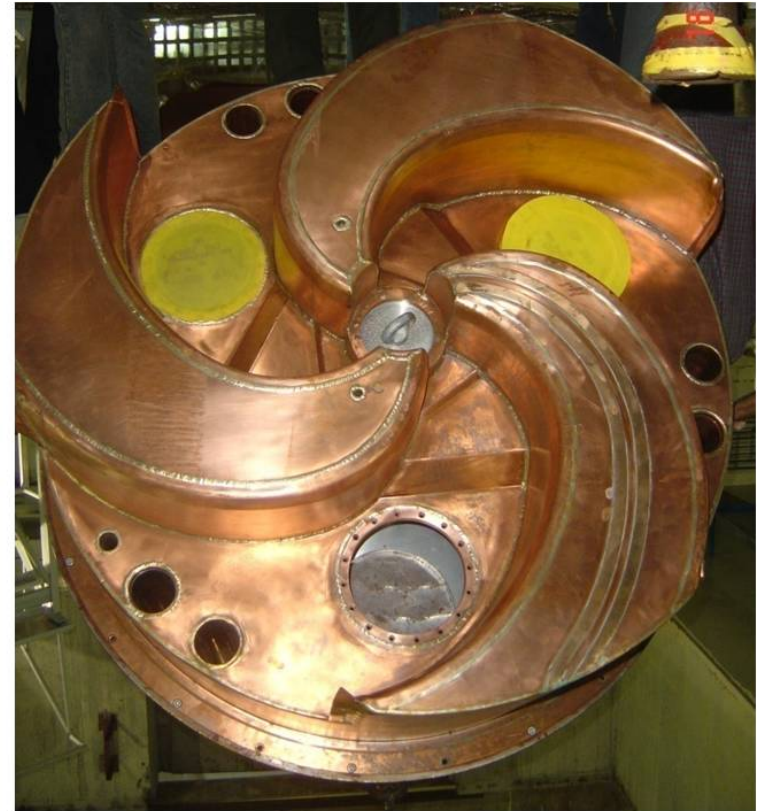
- $Q_0 = 4900$
- Variation of Quality factor (Q_0) :
Measured value is $\sim 28\%$ down
from simulated value



INSTALLATION OF TRIM COILS AND RF LINER



Trim Coils



Lower RF Liner

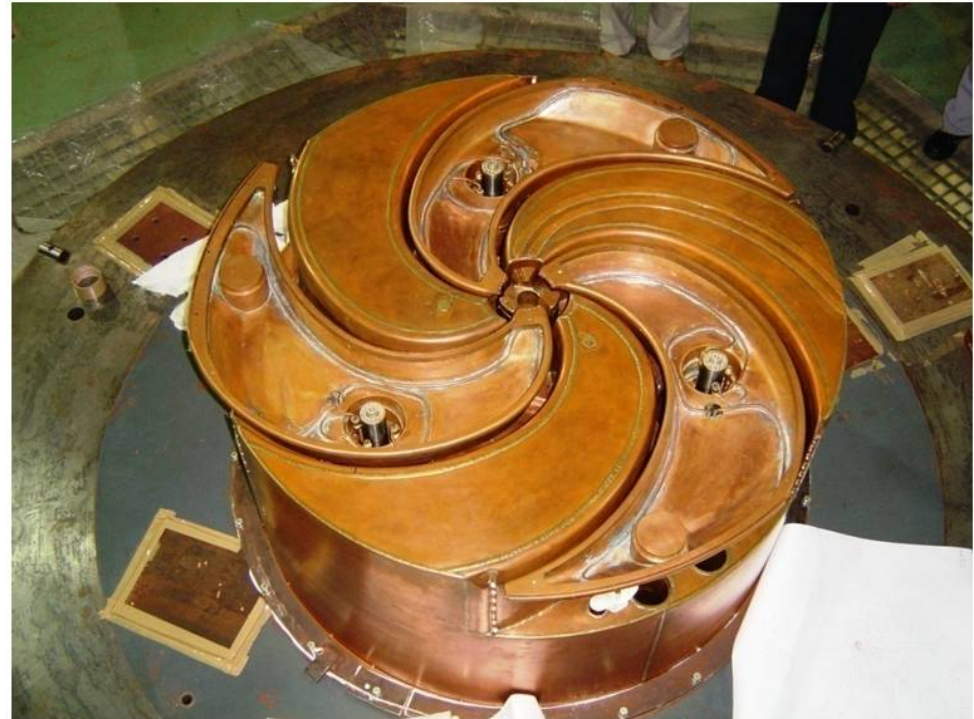
ASSEMBLY OF RF SYSTEMS



Dee



Outer conductor spinning



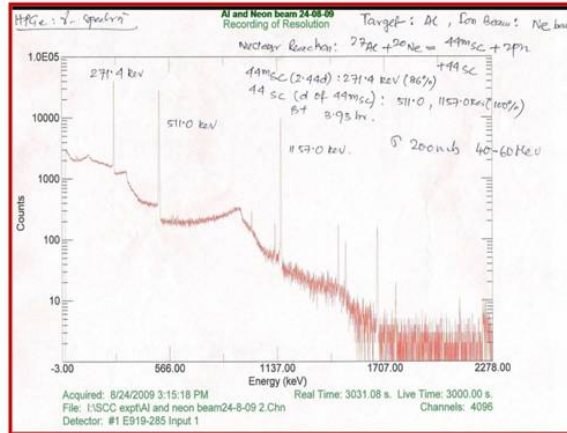
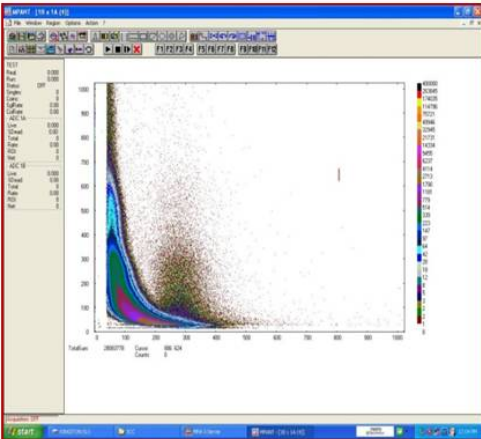
14 GHZ ECRIS AND LEPT COMMISSIONING



SC CYCLOTRON ACCELERATES INTERNAL BEAM



Beam current profile along radius

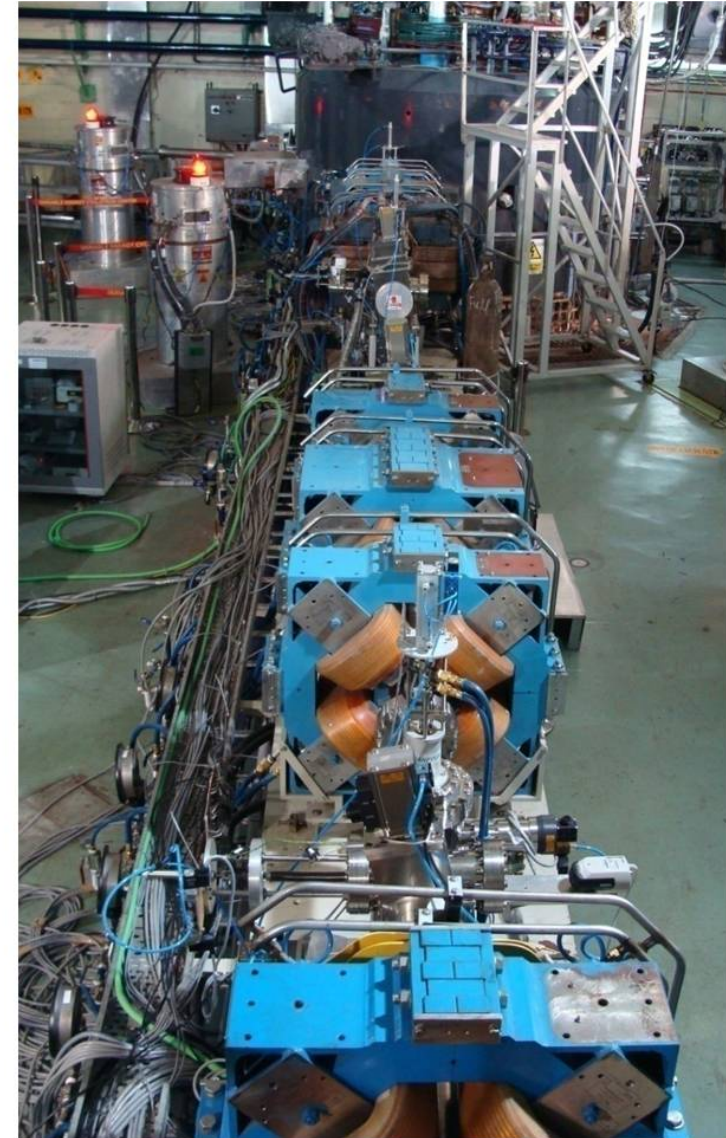


Neutron and gamma spectrum from (Ne + Al) nuclear reaction



Beam spot on ZnS plate

SUPERCONDUCTING CYCLOTRON WITH EXTRACTION BEAM LINE





DIAGNOSIS OF THE BEAM EXTRACTION PROBLEM

- **Measurement of beam centering**
- **Measurement of beam phase w. r. t. RF**
- **Inflector rotation arrangement**
- **Magnetic field Mapping**
- **Dee voltage measurement**
- **Improvement in RF Phase stability**

RF VOLTAGE MEASUREMENT USING CDTE X-RAY DETECTOR



Dee

Liner

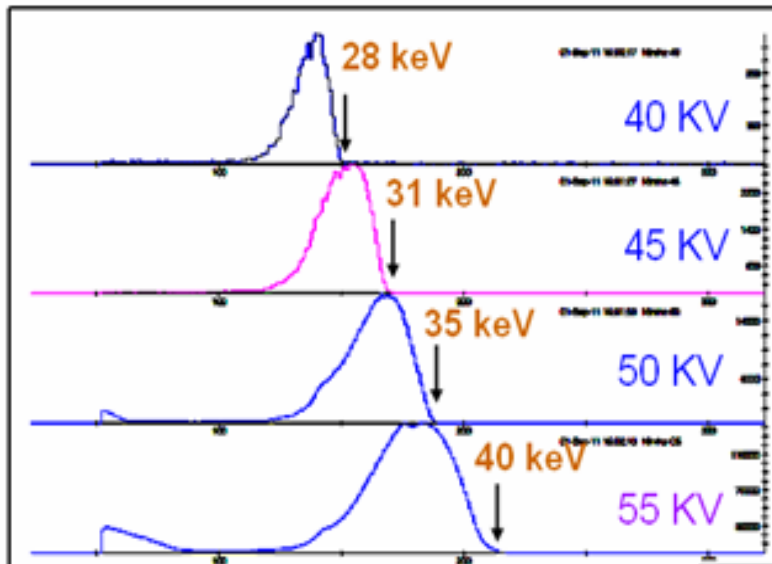


Port for inserting X-ray detector



X-RAY DETECTOR

DEE VOLTAGE MEASUREMENTS

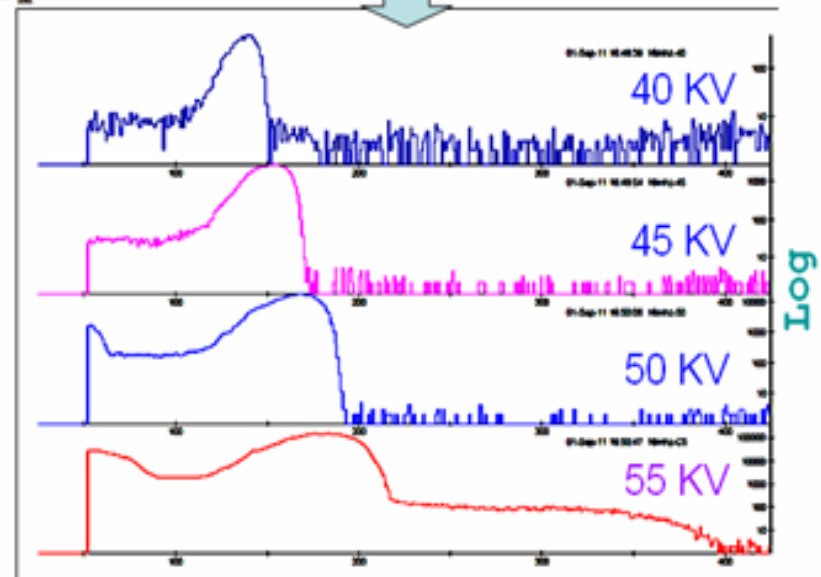


The **End point** has been “chosen” in the **linear** plot as the end of the “semi Gaussian” shape.

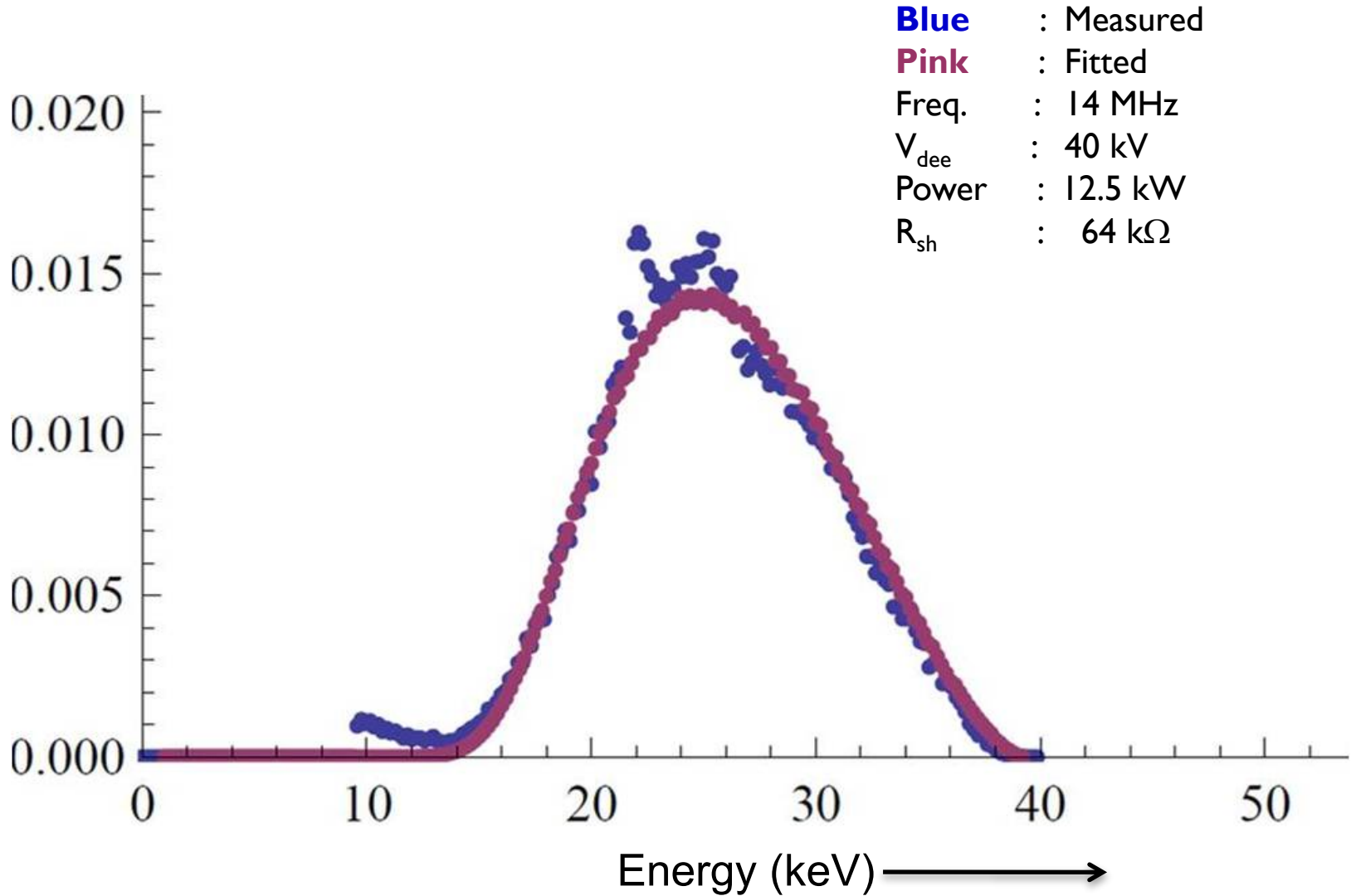
The data were taken for about **5 – 10 min** duration each except for the **55 KV** data which has been taken for **4 hrs**.

The spectra look some what different in semi-Log plot.

Use of Bremstrahlung technique to determine the actual dee voltage. This measurement is very important as asymmetry in dee voltage leads to deterioration in beam quality by inducing coherent oscillation in the beam.



BREMSSTRAHLUNG SPECTRUM



IMPROVEMENT OF RF PHASE STABILITY

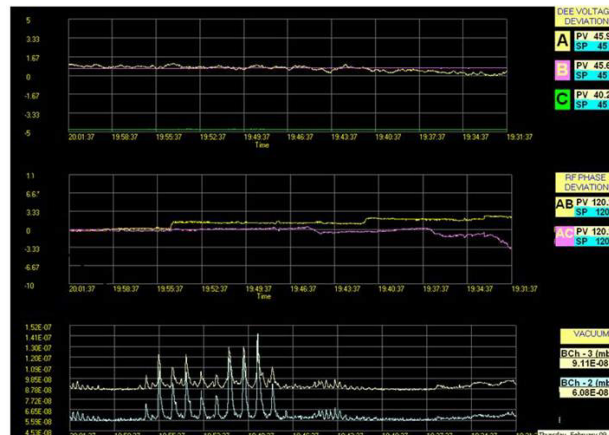
- Previously Phase Stability was $\pm 0.5^\circ$ to 1° .
- New phase control loop based on Direct Digital Synthesis (DDS) technique achieved stability within $\pm 0.1^\circ$.

Earlier:

RF Voltage

RF Phase

Vacuum



Analog Phase Regulator



Now:

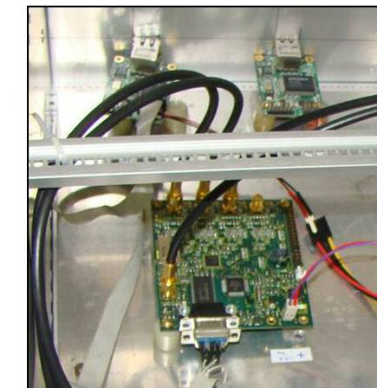
RF Voltage

RF Phase

Vacuum



Digital Phase Regulator



Dee voltages & Phase plots (at 14 MHz) Vs. time

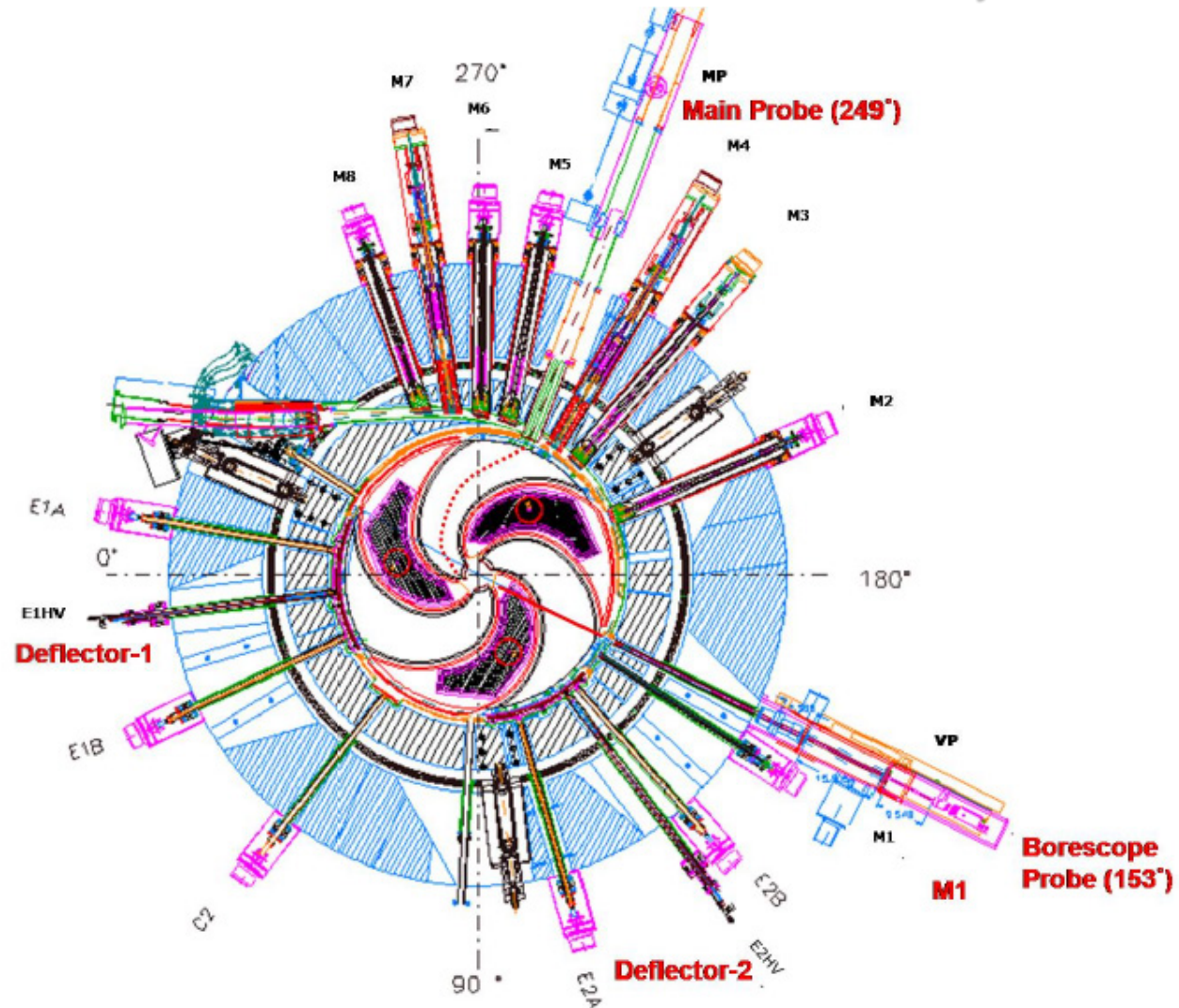
BEAM CENTERING MEASUREMENT WITH THREE PROBES BY SHADOWING TECHNIQUE

Median Plane Sectional View of SC Cyclotron:

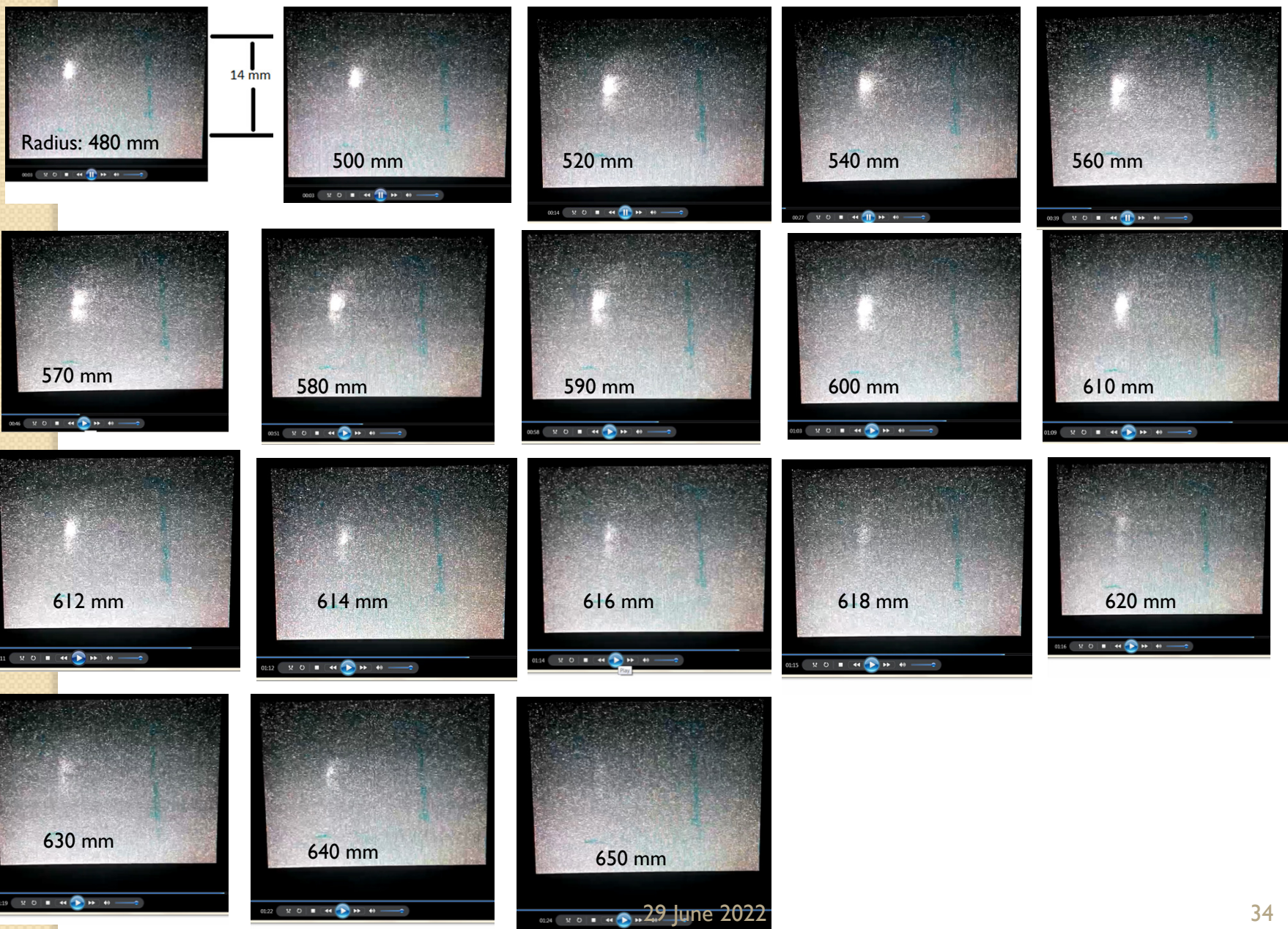
Observation:

Beam gets off-centered after 600 mm radius

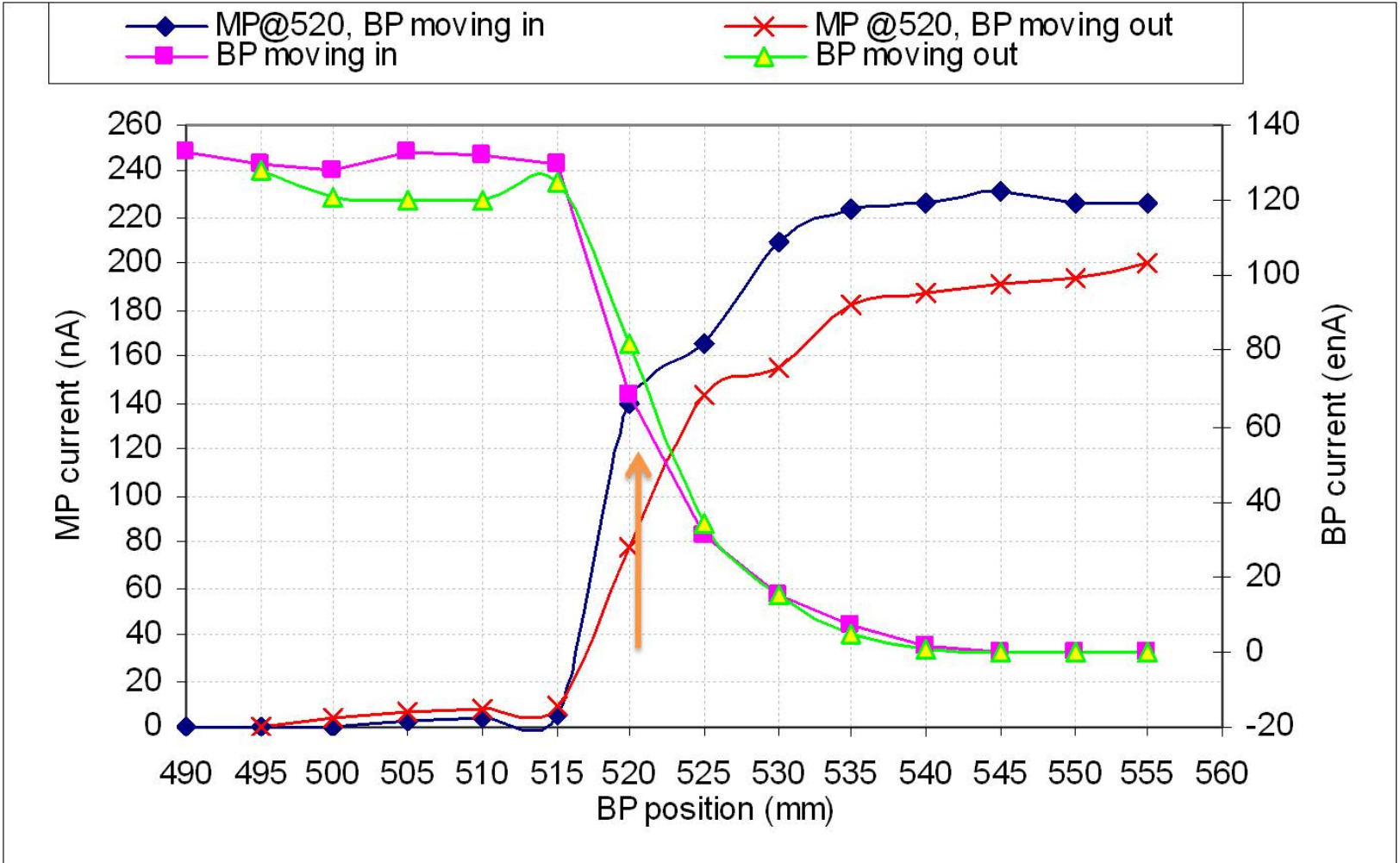
Deflector position at 667 mm



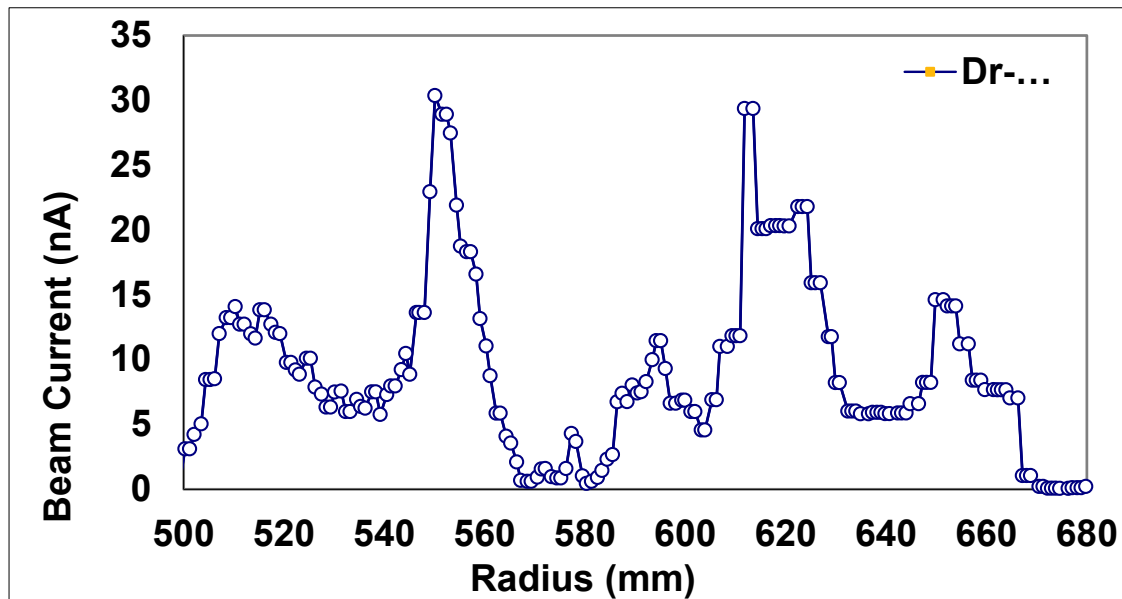
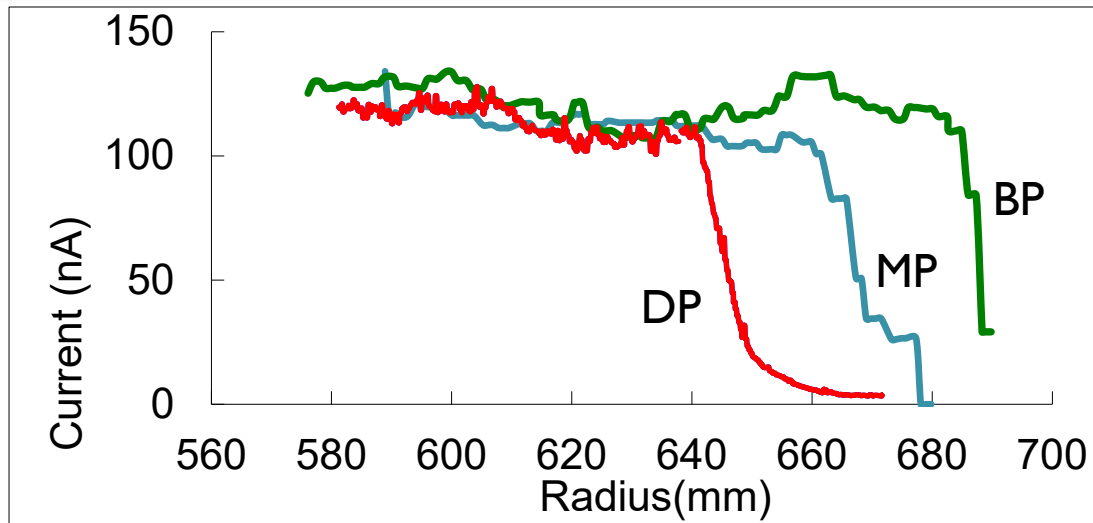
SNAPS FROM A MOVIE OF THE BEAM SPOT AS THE BOROSCOPE PROBE MOVES OUT. THE RADIAL STAMPINGS ARE WRITTEN. EXTRACTION RADIUS = 667 MM



ORBIT CENTERING MEASUREMENT BY SHADOWING METHOD



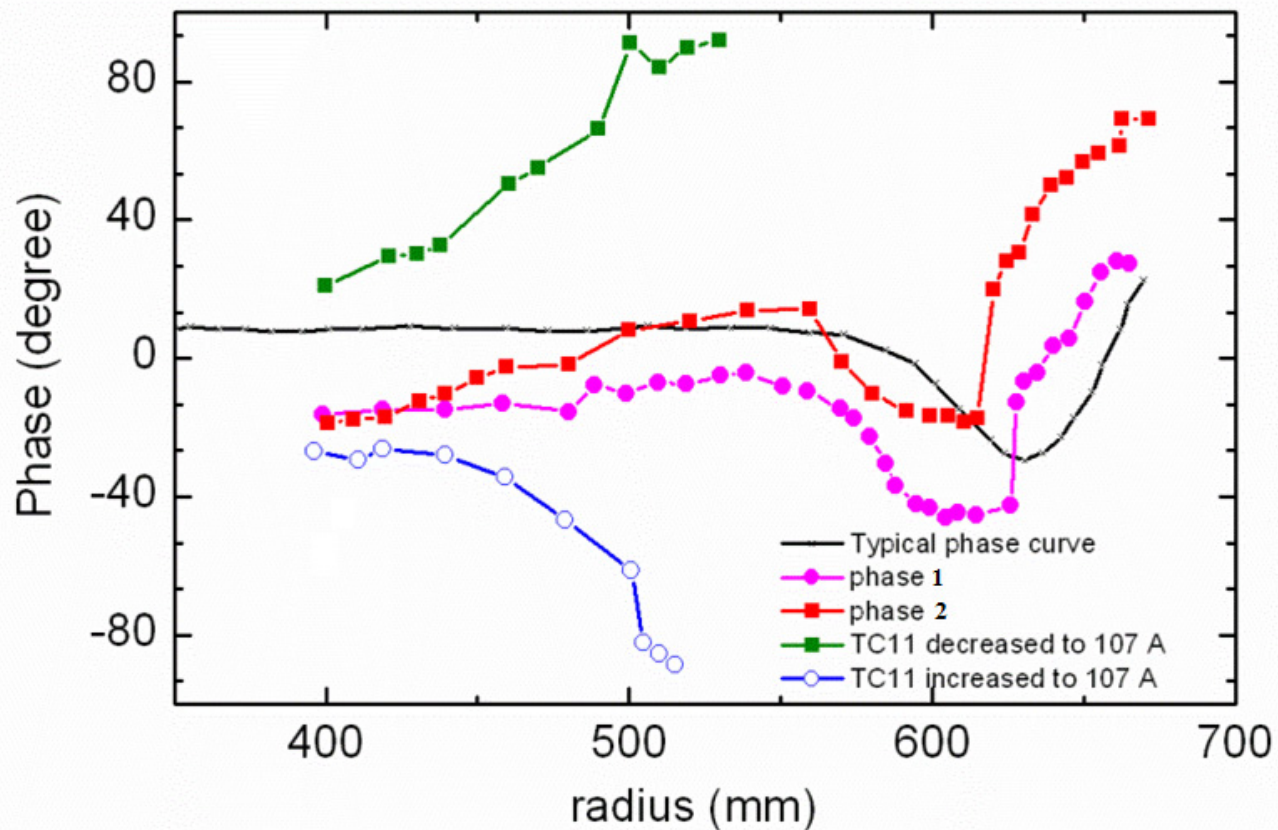
- Three beam current probes: Main probe (MP), Boroscope probe (BP), Deflector probe (DP)
- Differential (Dr) Probe



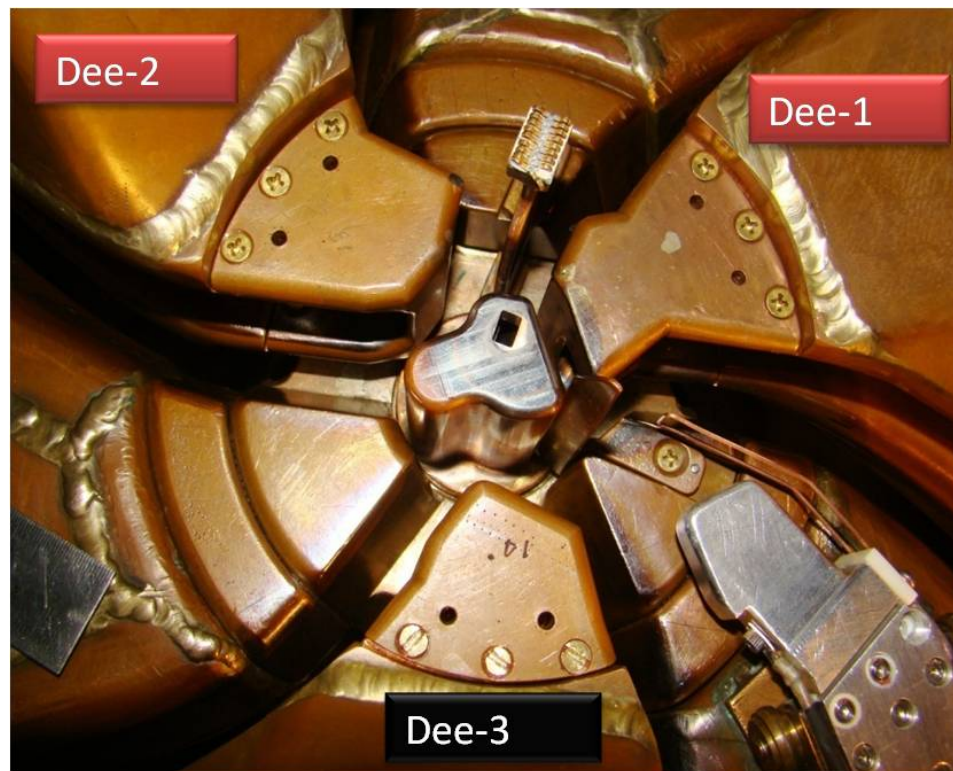
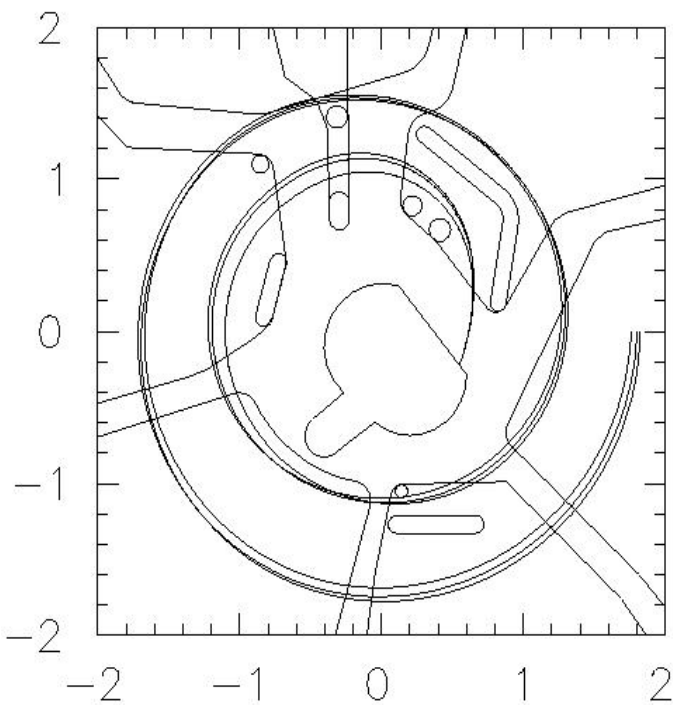
PHASE MEASUREMENT

Smith and Garren Method

- RF Frequency Detuning
- Field Detuning

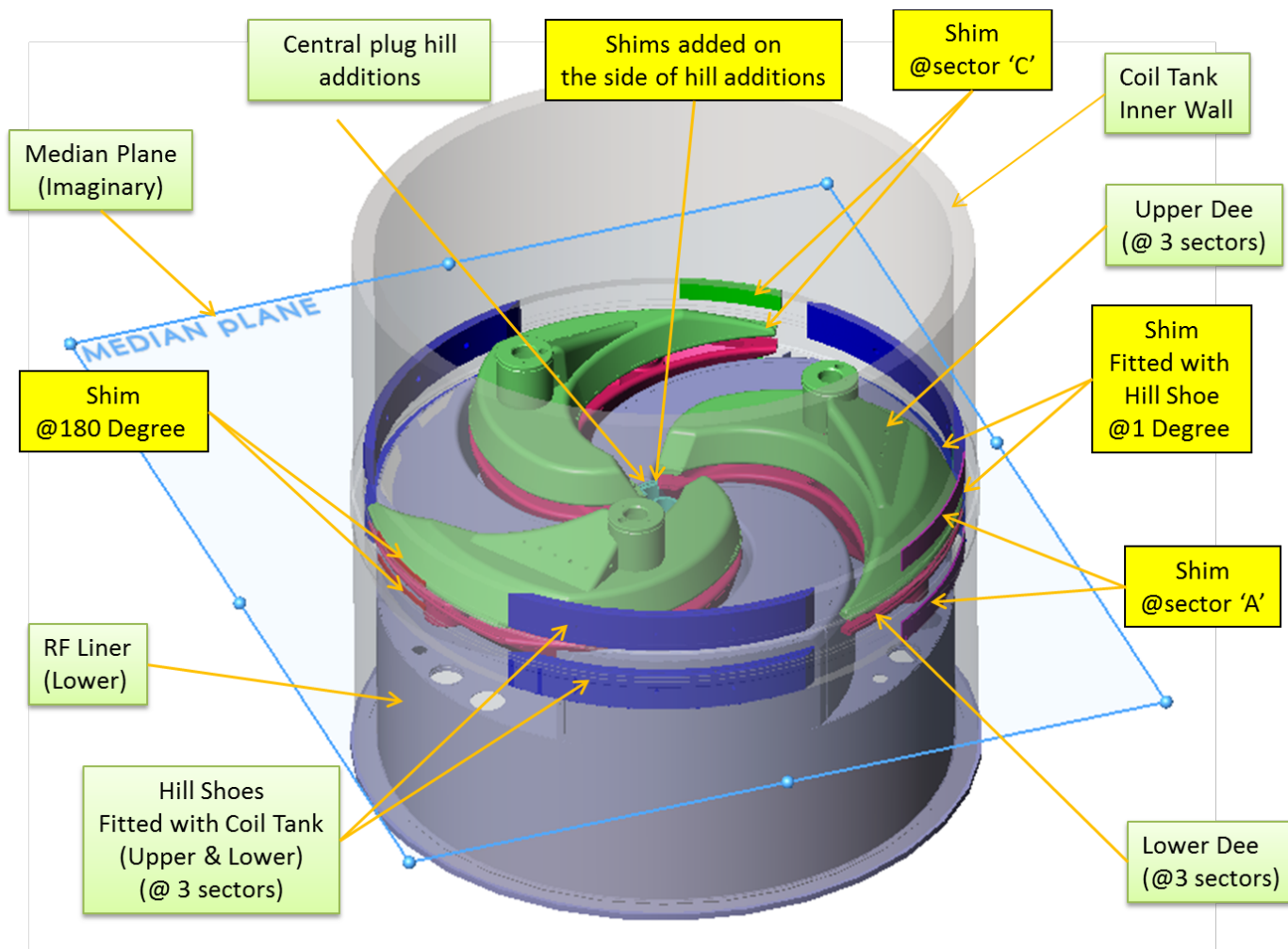


CENTRAL REGION GEOMETRY MODIFICATION

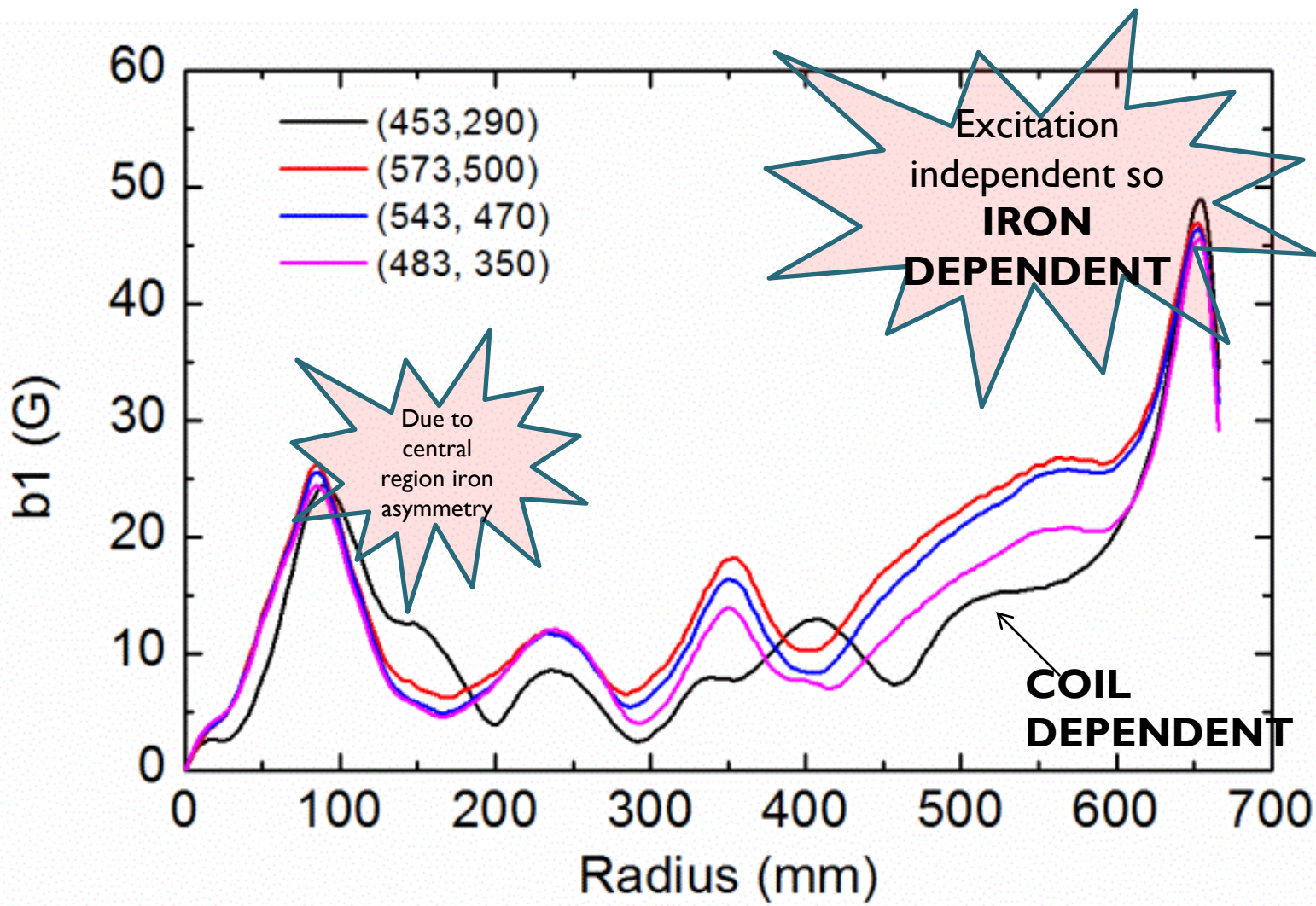


PARTIAL CORRECTION OF 1ST HARMONIC BY IRON SHIMS

Shifting of coil tank would require complete disassemble of the magnet. So field correction in only limited excitation of the coils was attempted by **putting iron shims on the coil tank walls in the valley regions.**

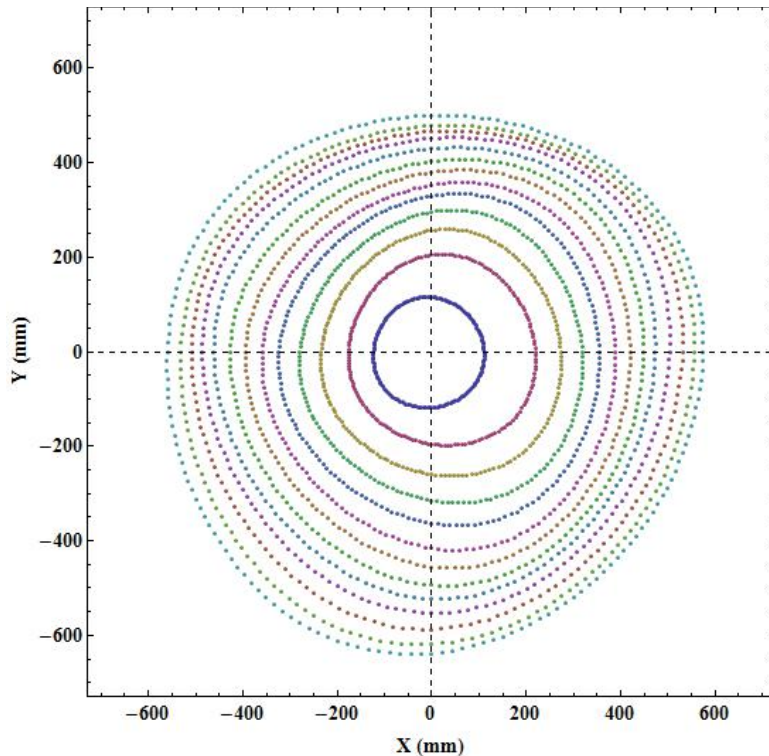


SOURCE OF FIRST HARMONIC



INFLUENCE OF FIRST HARMONIC FIELD IMPERFECTION

- Beam off-centering in central & extraction region is more dangerous near $V_r = 1$ resonance
- Deflector geometry and position may not be matching with beam trajectory



Equilibrium orbit in presence of first harmonics

$$x'' + \nu_r^2 x = \frac{b_1}{B_{av}} \cos(\theta + \varphi)$$

Radial shift of orbit center,

$$\Delta x = \frac{b_1 R_{av}}{B_{av} (\nu_r^2 - 1)}$$

- Amplitude of first harmonics (b_1)
- Orbit Avg. radius (R_{av})
- Operating average field (B_{av})



OBSERVATIONS FROM EARLIER FIELD MAPS

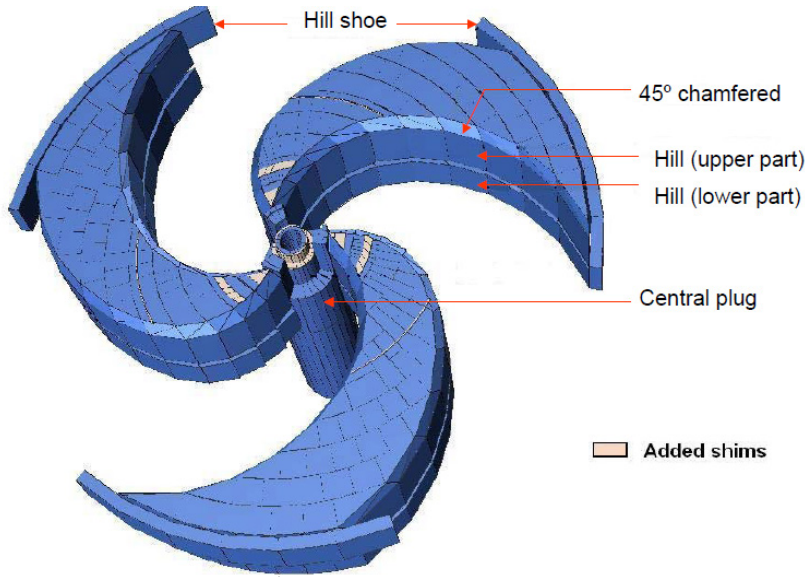
Observations:

- First harmonic profiles are dependent on excitations of alpha and beta coils (left figure)
- Radial position of first harmonic peak near extraction is independent of excitation
- The phases of first harmonic peaks (about 650 mm) at different excitation lies between 150 to 165 degree (w.r.t. cyclotron coordinate system, angle increasing anti-clockwise)
- Peak value changes with excitation (within about 10 Gauss in the range of our maps)
- First harmonic peak near centre (~100 mm) is independent of coil excitations

Comments:

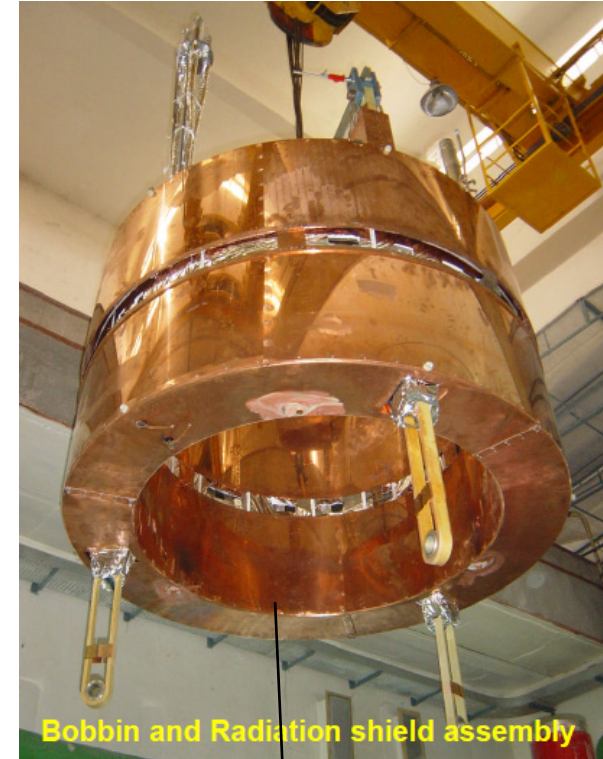
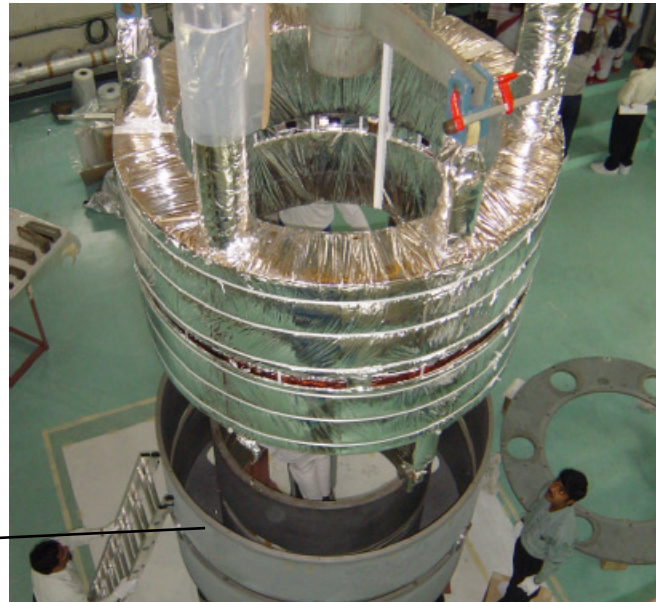
- the changing profiles of first harmonic with current indicates **coil-shift radially**
- Fixed peak position indicates a major contribution to this peak from iron part (possible candidates: coil-tank, hill-shoe, pole-tip edge etc.)
- The peak near centre was found due to errors in the local iron parts, which has been rectified.

CORRECTION: CENTRAL PLUG AND COIL-TANK



HILL SHOE
 ATTACHED TO
 COIL TANK

COIL TANK



Bobbin and Radiation shield assembly

COIL

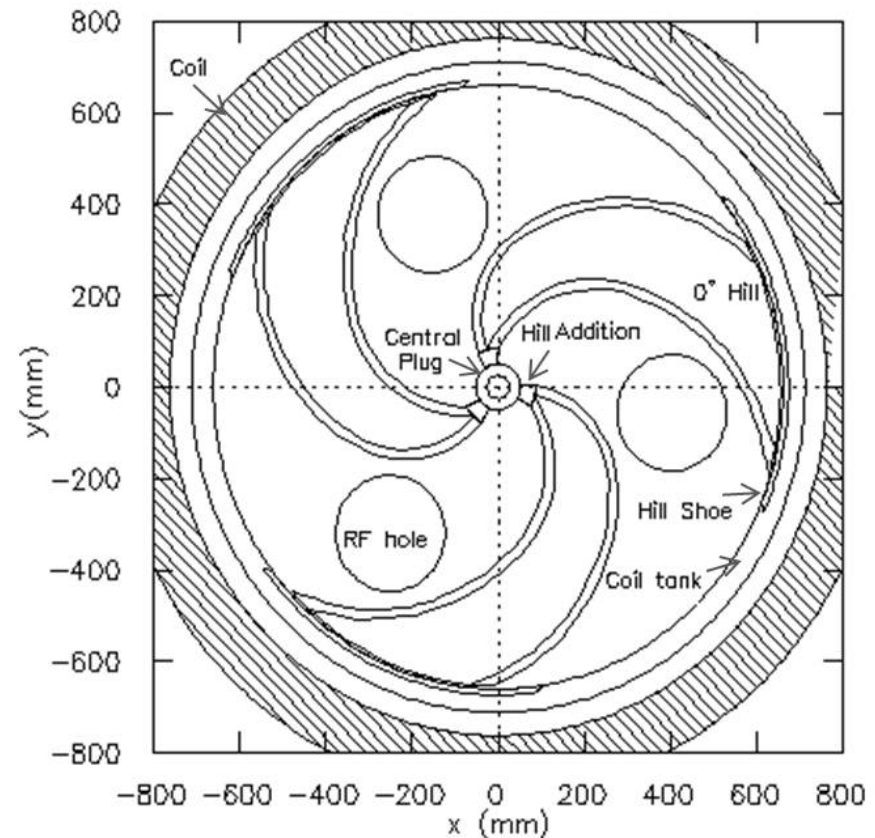
About Main Magnet

SOURCES OF MAGNETIC FIELD IMPERFECTIONS: POSITIONING ERROR OF COILS AND CRYOSTAT

pole radius 654.05 mm
Central plug radius 88.9 mm
50.8 mm diameter central hole

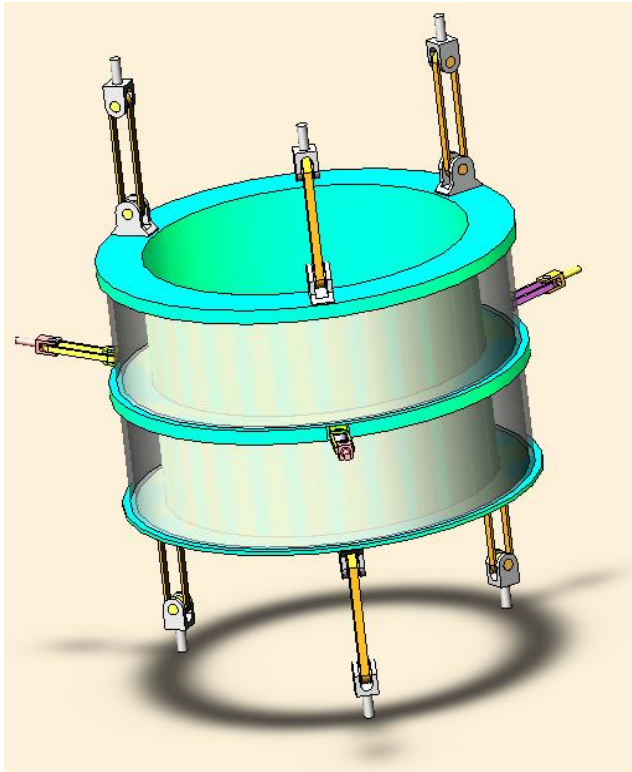
Hill width 33° (inside) to 46° (outside)
 'hill-shoe' 60° wide
 'hill-addition' from 50.8 mm to 88.9 mm

Plan view of the K500 cyclotron



FIELD IMPERFECTIONS DUE TO CRYOSTAT POSITIONING ERROR:

Schematic diagram of the support links and the bobbin/liquid helium chamber

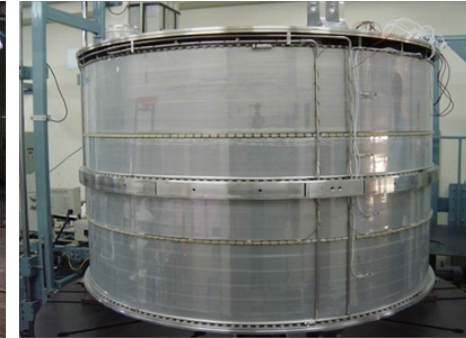


The positioning of the main coils is essentially a compromise between the balancing of magnetic force on the support links and the field imperfections.

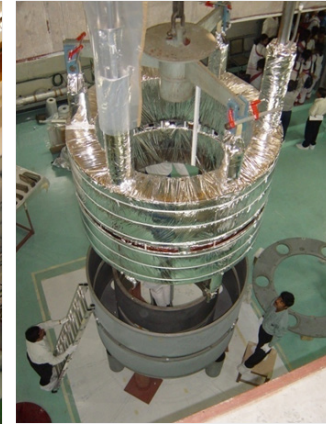
bobbin



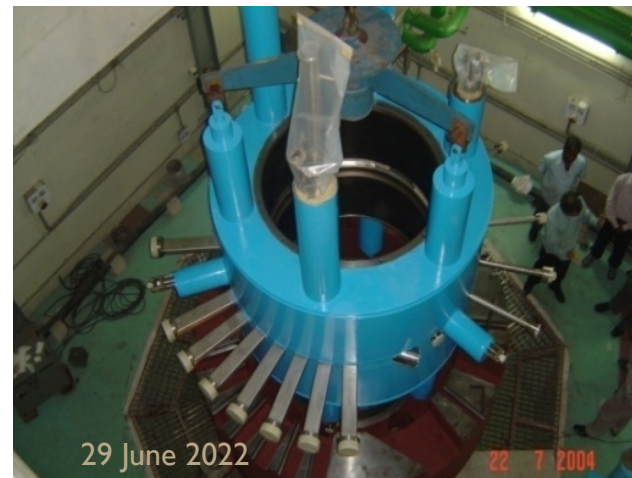
coils



LN shield

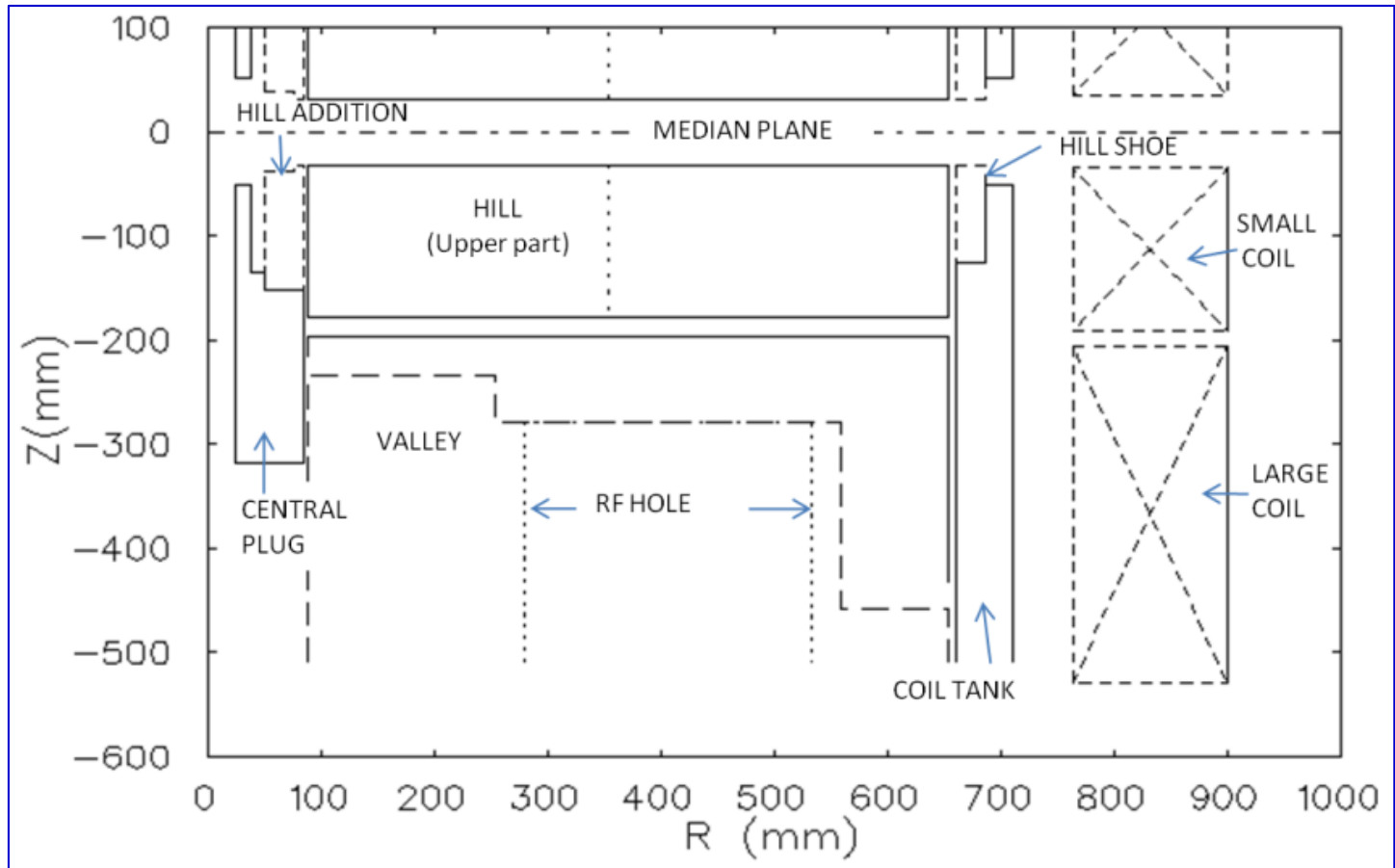


Multi Layer insulation



radial penetration ports, LN and LHe supply and return ports and current lead port fitted to the enclosed vacuum chamber

Vertical sectional view through a spiral line along the hill centre, superimposed on a sectional view along the valley centre



**coils extend from 763.7 mm to 900.4 mm radius median plane at $z = 0$,
 Small coil extends from $z = 35.3$ mm to 191.2 mm
 Large coil extends from $z = 206.7$ mm to 529 mm**



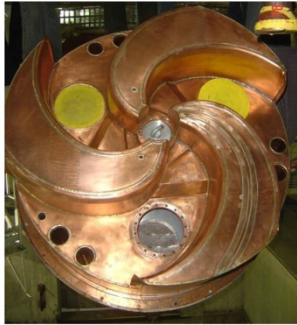
DE-ASSEMBLE THE MAGNET:

Cryostat is brought down in the **annular space** between pole and yoke

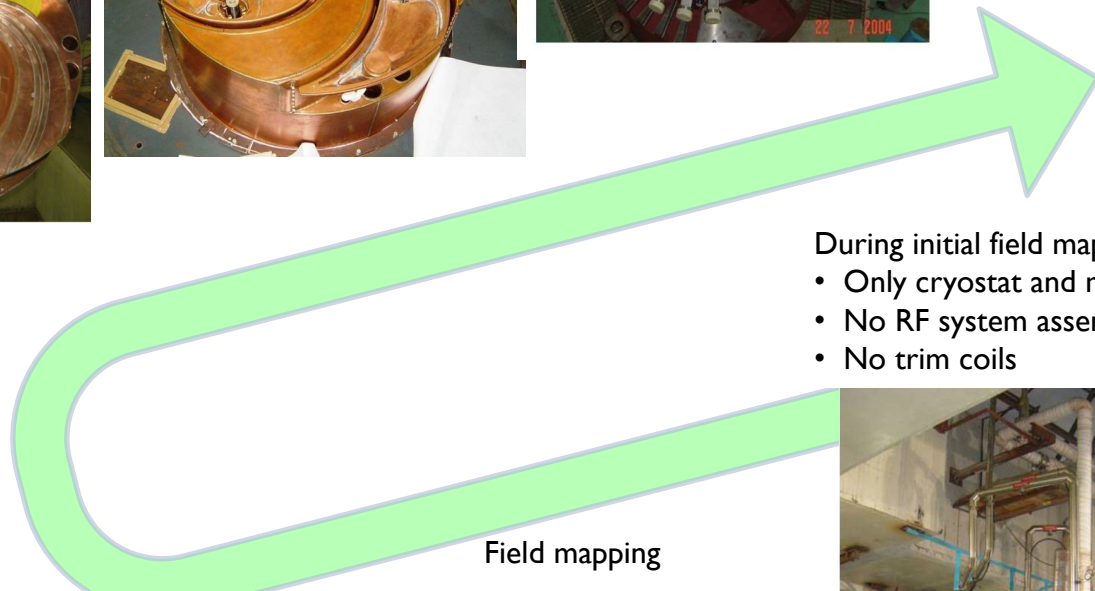
Dees assembled

Liner are capped over pole assemble
Gap 18 mm

Trim coils wound around pole-tips



Upper pole is put on

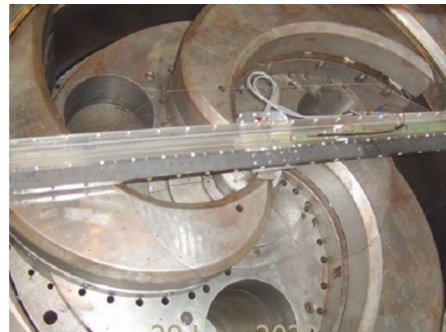


- During initial field mapping
- Only cryostat and magnet iron
 - No RF system assembly
 - No trim coils



Magnet disassembled

Bare pole-tips
63 mm gap



29 June 2022

Field mapping



COIL-TANK POSITIONING



New coil tank positioning mechanism : allows precise positioning of the cryostat

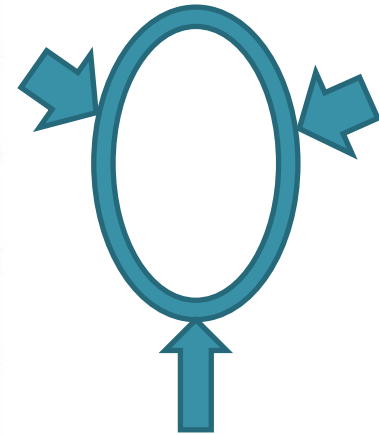
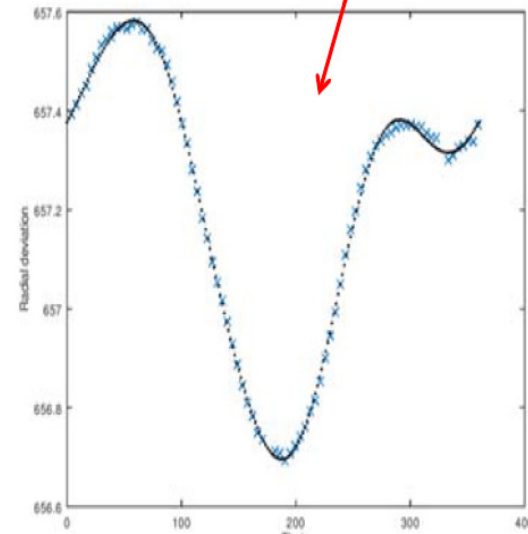


Measurement with CMM

Radial deviation of cryostat w.r.t. central plug centre as a function of angle after final repositioning : Max. deviation 0.35 mm at 15°



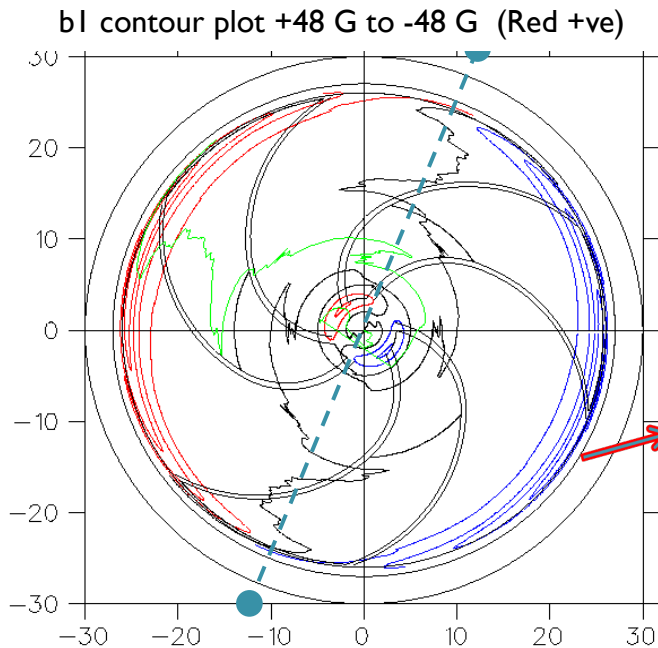
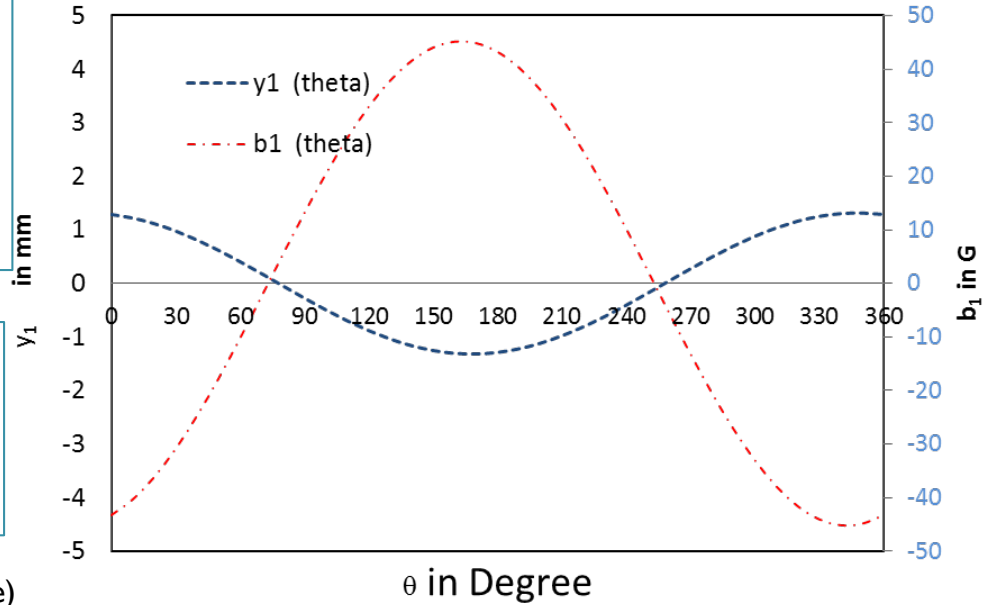
Field mapping Jig



Coil-tank ID deviation graph

• **From magnetic field map**, Cryostat is shifted 1mm w.r.t. cyclotron axis along **336 ± 3** degree

• Cryostat to be shifted w.r.t. cyclotron axis by **1 ± 0.1** mm along **156 ± 3** degree



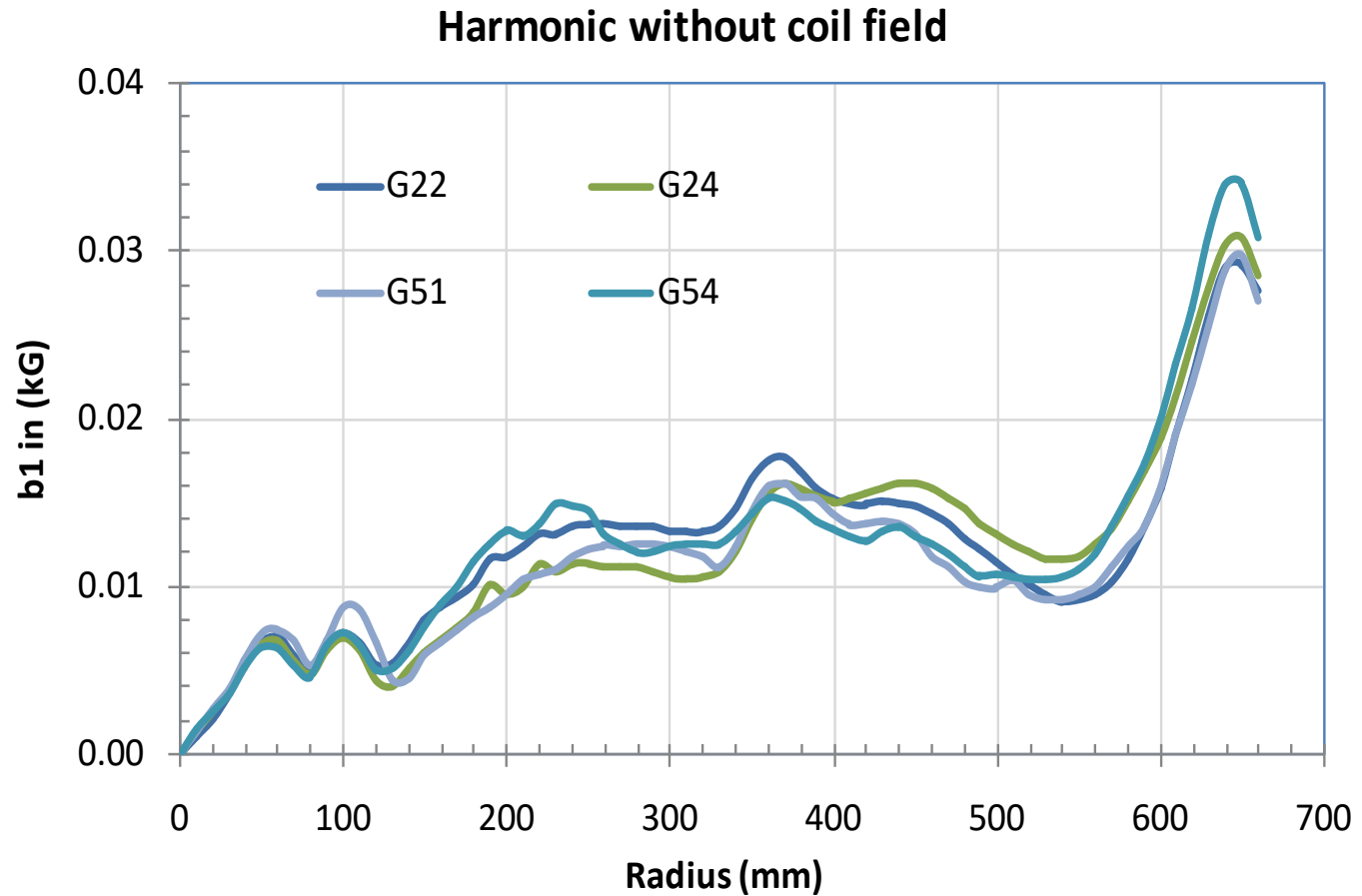
Contour plot of 1st harmonic field error (before correction)

Coil_Tank shifted along 336 deg.

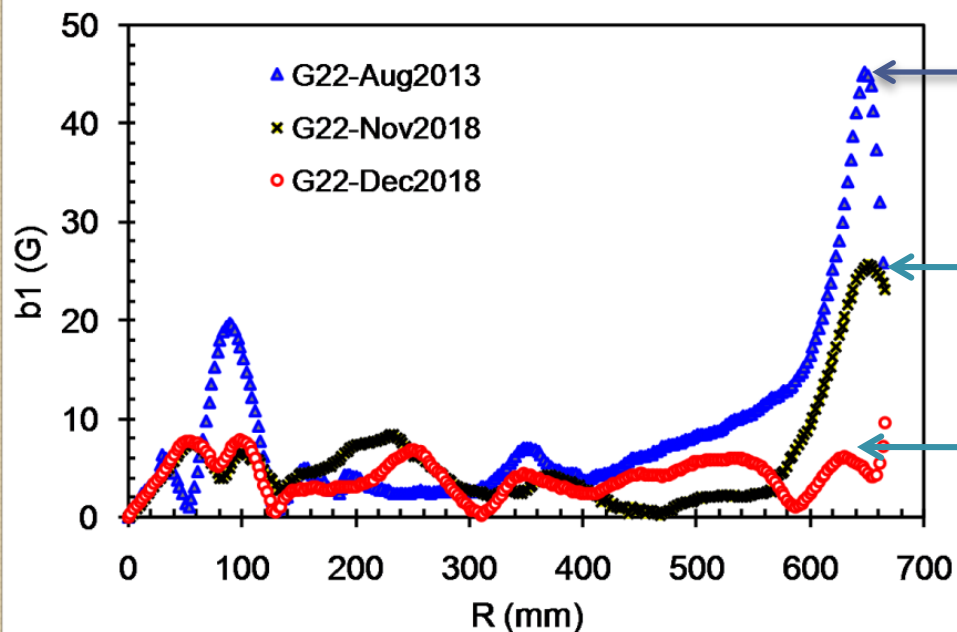
MAGNETIC FIELD MAP (AFTER 1ST STEP OF COIL TANK SHIFT)

At 650 mm radius $b_1 \sim 30$ G (Reduced but not as required)

1st harmonic field amplitude Subtracting coil-shift effect



CORRECTION OF FIRST HARMONIC FIELD IMPERFECTION IN SCC



Before Correction
($b_1 > 45\text{G}$)

After central plug correction & first cryostat repositioning

After final cryostat repositioning within $\pm 0.1\text{mm}$ accuracy
($b_1 < 10\text{G}$, desirable)

Mismatch between magnet centre and cryostat centre ($\sim 1\text{ mm}$)
(established by **simulations** and also **measurement**)

Step 1: Shimming in sector 'C' at 65 mm to correct central region 1st Harmonic

Step 2: Central plug correction

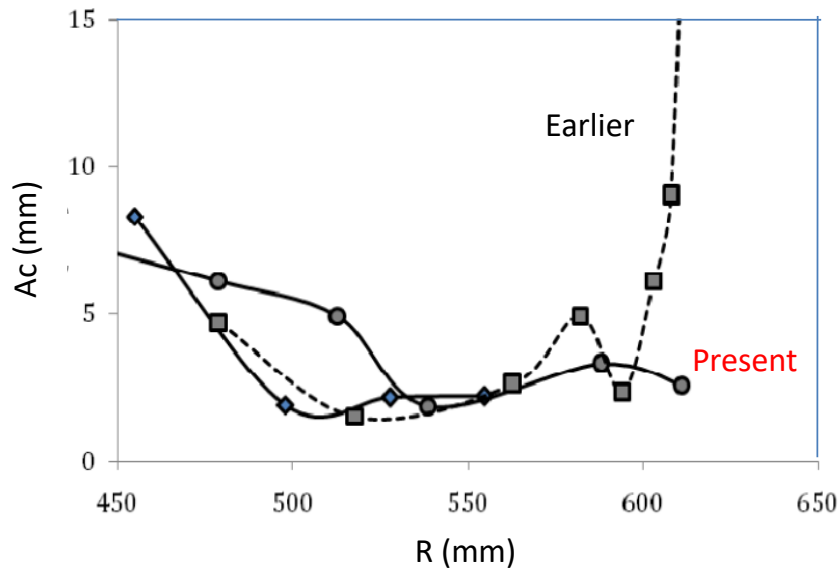
Step 3: Coil tank repositioning to correct extraction region 1st Harmonic

Step 4: Coil repositioning followed by coil tank

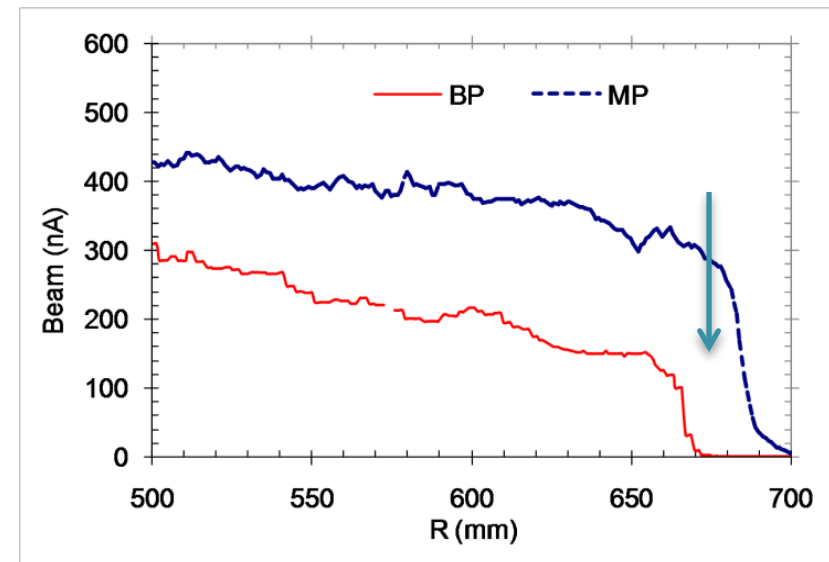
IMPROVEMENT OF BEAM QUALITY AFTER MAGNETIC FIELD CORRECTION

- ❖ Tuning started at 14 MHz RF, Ion N^{2+} , 4.5 MeV/A, $h=2$
- ❖ After the correction of magnetic field, Beam current has increased
- ❖ Beam Centering has improved As Seen from shadow measurement

Coherence oscillation amplitude



Beam Profiles in Probes

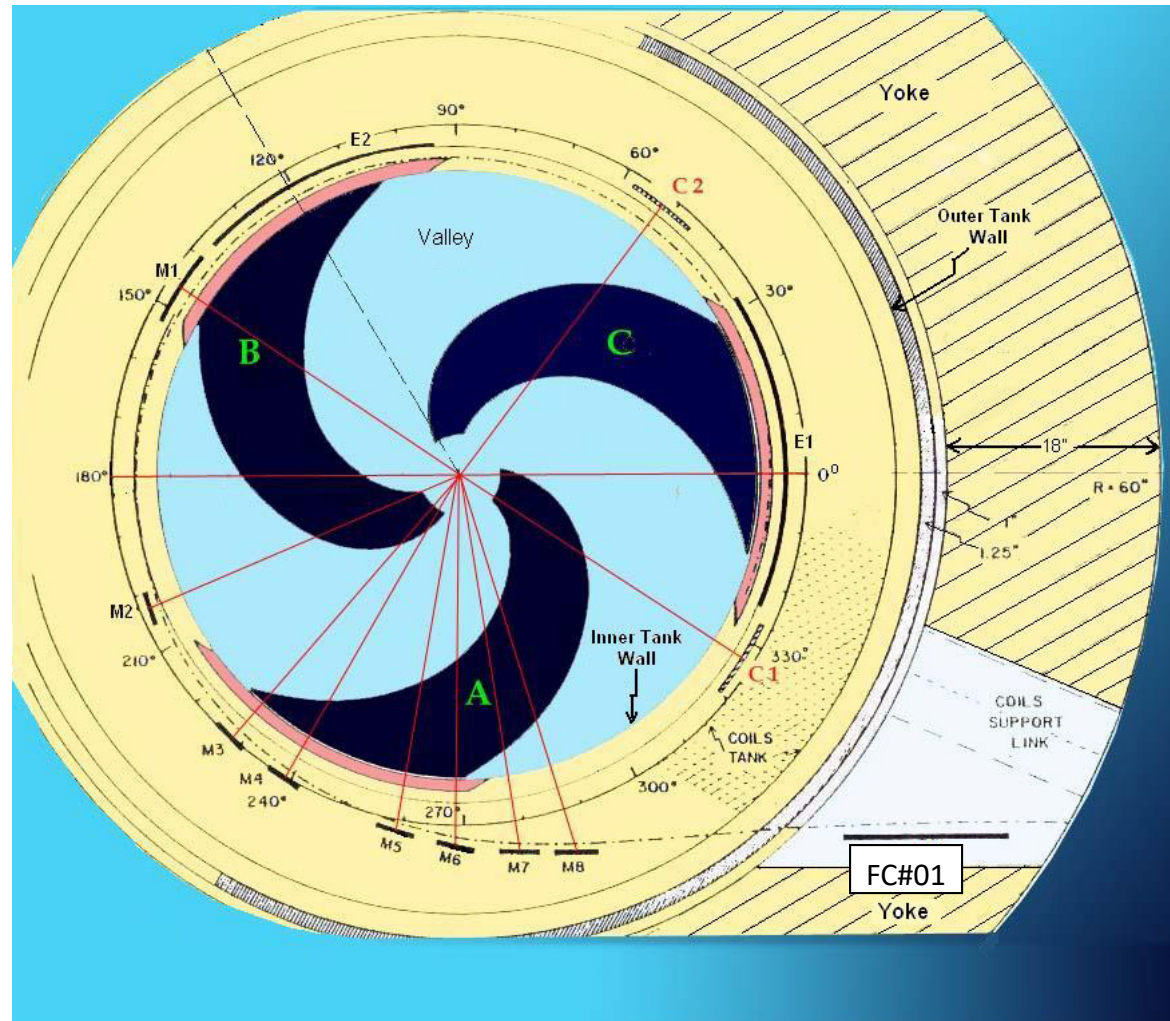


EXTRACTION SYSTEM OF SUPERCONDUCTING CYCLOTRON

- Two Electrostatic Deflectors
- 8 passive Magnetic Channels
- 1 Active magnetic channel

Beam Extraction from SCC

- N²⁺ beam (4.5 MeV/A) extracted through the deflectors, magnetic channels, up to the Target.



BEAM ON THE ZNS SCREEN

Earlier

Present

Radius 600 mm



Radius 600 mm



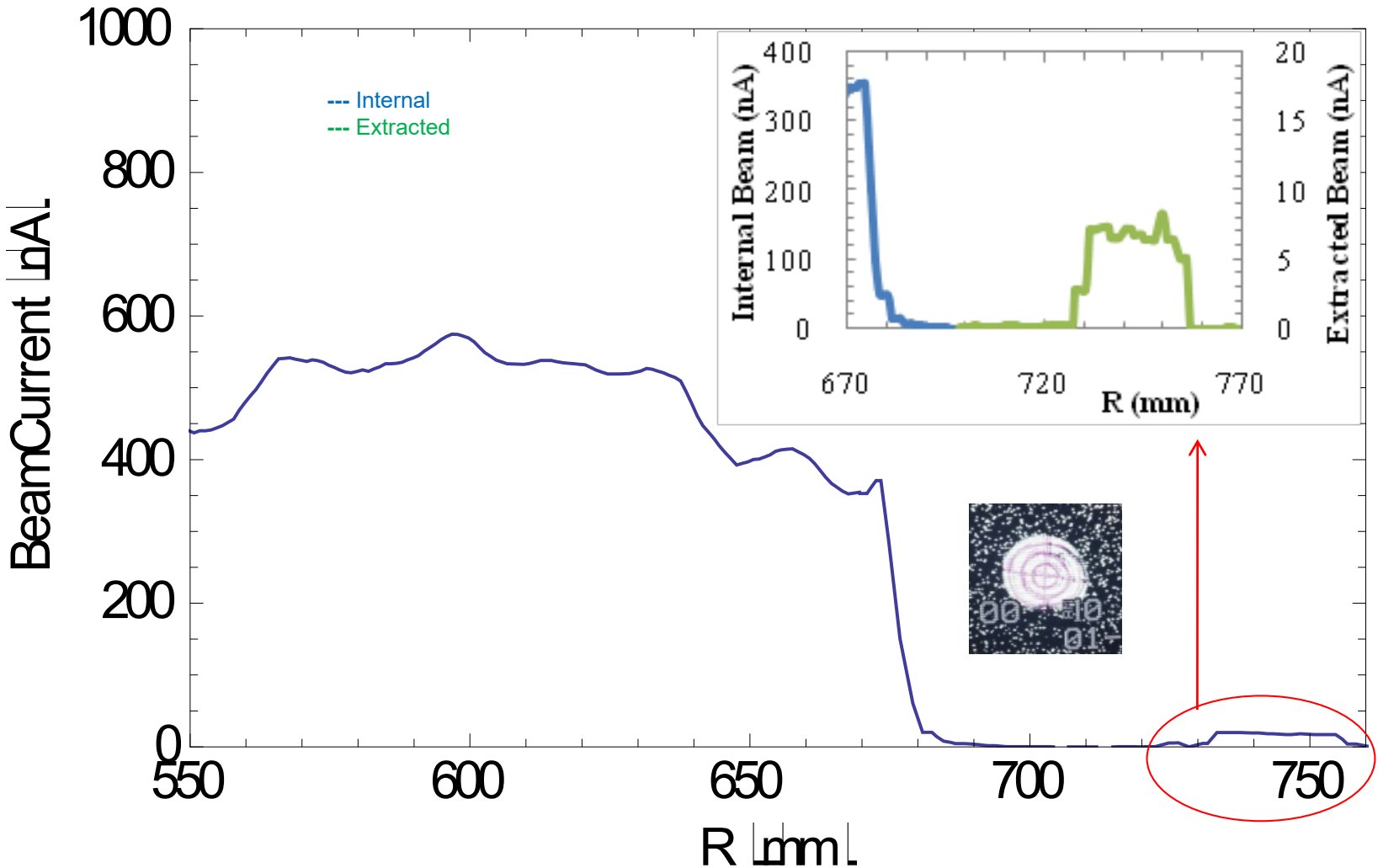
Radius 625 mm



Radius 660 mm



EXTRACTED AND INTERNAL BEAM PROFILES FOR N^{2+} , 4.5 MEV/A, 14 MHZ RF, H = 2, DEE VOLTAGE ~ 30 KV





BEAM ON FIRST FARADAY CUP OUT SIDE THE CYCLOTRON

| #PS | Actual Value | Set Value | Interlock | Polarity | Status |
|-----------|--------------------|-----------|-----------|----------|--------|
| TCPS #0 | 12.52 | 12.50 | OK | +ve | ON |
| TCPS #1A | 90.12 | 90.10 | OK | +ve | ON |
| TCPS #1B | 119.51 | 119.50 | OK | +ve | ON |
| TCPS #1C | 163.66 | 163.66 | OK | +ve | ON |
| TCPS #2 | Switched OFF / ... | | | | |
| TCPS #3 | -0.02 | 0 | OK | +ve | OFF |
| TCPS #4 | -5.78 | -5.8 | OK | +ve | ON |
| TCPS #5 | -158.53 | -158.5 | OK | -ve | ON |
| TCPS #6 | -120.95 | -121 | OK | +ve | ON |
| TCPS #7 | -224.84 | -224.8 | OK | +ve | ON |
| TCPS #8 | -150.06 | -150.1 | OK | +ve | ON |
| TCPS #9 | -119.19 | -119.2 | OK | +ve | ON |
| TCPS #10 | -8.11 | -8.1 | OK | +ve | ON |
| TCPS #11 | -127.01 | -127 | OK | +ve | ON |
| TCPS #12 | -225.39 | -227.1 | OK | +ve | ON |
| TCPS #13A | 8.63 | 8.60 | OK | +ve | ON |



BEAM ON TARGET

172.24.5.150 - Remote Desktop Connection

Multiplexed Current

Magnetic Channels

| | | |
|-------|-----------|--------------|
| MC 02 | MC 03 | MC 04 |
| +9.9 | +9.9 | +2.86 |
| MC 05 | MC 06 | MC 07 |
| +9.89 | +0.58 | -0.02 |
| MC 08 | MC 09 Top | MC 09 Bottom |
| +9.9 | +0.07 | +0.18 |

All currents in **nA**

Vault

| | | | |
|-------|-------|-------|-------|
| FC 01 | FC 02 | FC 03 | FC 04 |
| -0 | -0 | -0.1 | -0 |

Cave

| | | | |
|--------------|-------------|--------------|-------------|
| FC 05 | FC 06 | Target FC | |
| +0 | -0.03 | +0.54 | |
| SLIT-X-Right | SLIT-X-Left | SLIT-Y-Right | SLIT-Y-Left |
| -0.68 | +0.9 | -0.64 | -0.67 |

NT LabVIEW 2013 (32-bit)

Windows taskbar: Type here to search, 7:55 PM, 1/23/2020

CS-Studio

DEFLECTOR-E1 Voltage (kV) **25.13** Current (uA) **36.337** ON OK REMOTE INTLCK VAC

Set Current (uA) **150.00** Set Voltage (kV) **25.20**

LOCK FINE COARSE LOCK FINE COARSE

Set current limit (uA) **80.0** Set time limit (sec) **1**

HALT RAMP to ZERO RAMP AUTO CONDITIONING ON OFF

DEFLECTOR-E2 Voltage (kV) **15.85** Current (uA) **2.930** ON OK REMOTE INTLCK VAC

Set Current (uA) **150.00** Set Voltage (kV) **16.35**

LOCK FINE COARSE LOCK FINE COARSE

Set current limit (uA) **80.0** Set time limit (sec) **1**

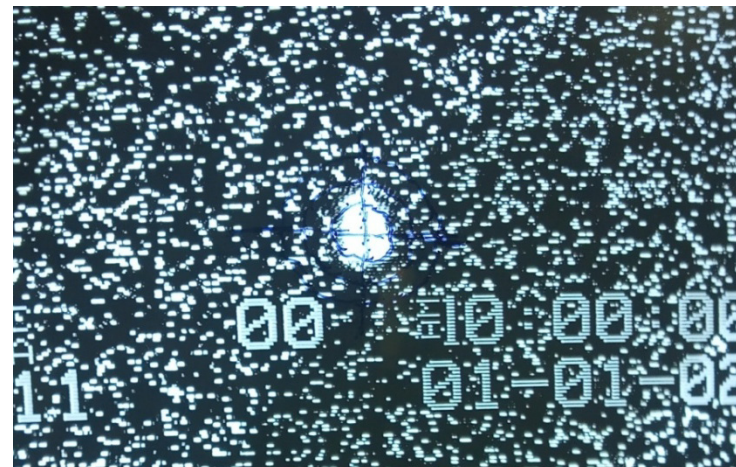
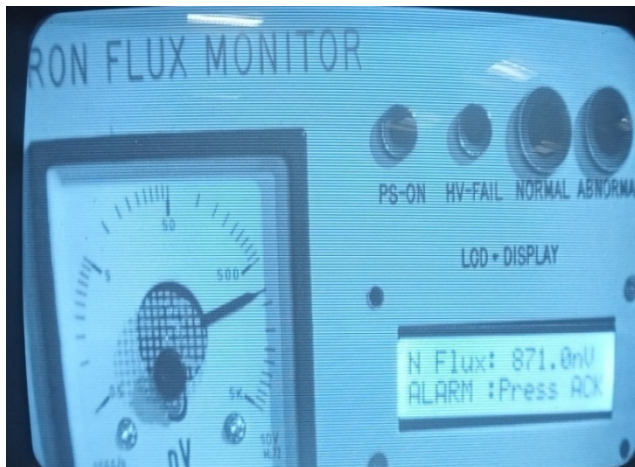
HALT RAMP to ZERO RAMP AUTO CONDITIONING ON OFF

TOP PAGE

Calculated Positions

Windows taskbar: 7:55 PM, 1/23/2020

BEAM ON TARGET



SCC Beam Diagnostics System (CAVE)

Scattering Chamber: -0.00

X SLIT: 24.9mm (L: -0.6, R: -0.7)

Y SLIT: 24.9mm (L: -0.6, R: -0.7)

Beam Viewer 6: IN, OUT

Beam Viewer 5: IN, OUT

Beam Viewer Camera: BV01, BV02, BV03, BV04, TARGET FC

Magnetic Channels:

| | | |
|---------------|---------------|------------------|
| MC 02: NC | MC 03: NC | MC 04: +3.3 |
| MC 05: +10.65 | MC 06: NC | MC 07: -0.02 |
| MC 08: NC | MC 09 Top: NC | MC 09 Bottom: NC |

Vault:

| | | | |
|--------------|--------------|--------------|--------------|
| FC 01: -0.01 | FC 02: -0.01 | FC 03: -0.04 | FC 04: +1.17 |
|--------------|--------------|--------------|--------------|

Cave:

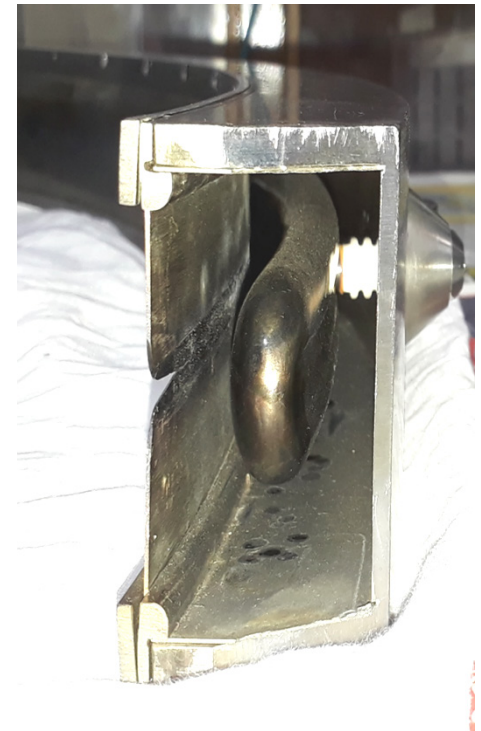
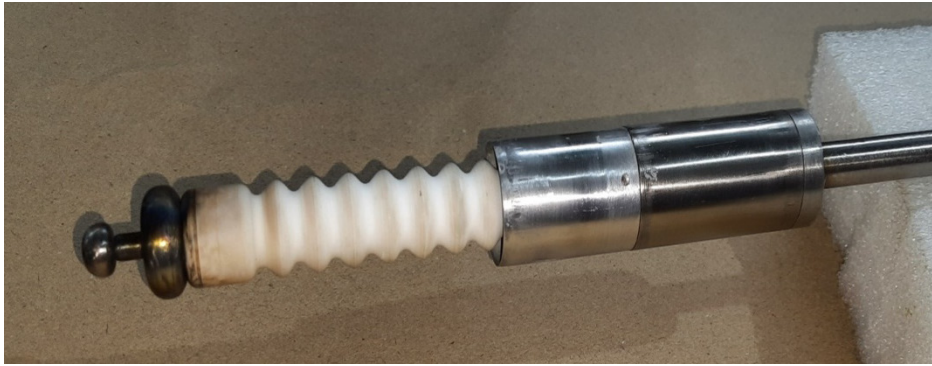
| | | | |
|---------------------|--------------------|---------------------|--------------------|
| FC 05: +8.36 | FC 06: +0.2 | Target FC: -0 | |
| SLIT-X-Right: -0.69 | SLIT-X-Left: -0.57 | SLIT-Y-Right: -0.66 | SLIT-Y-Left: -0.63 |



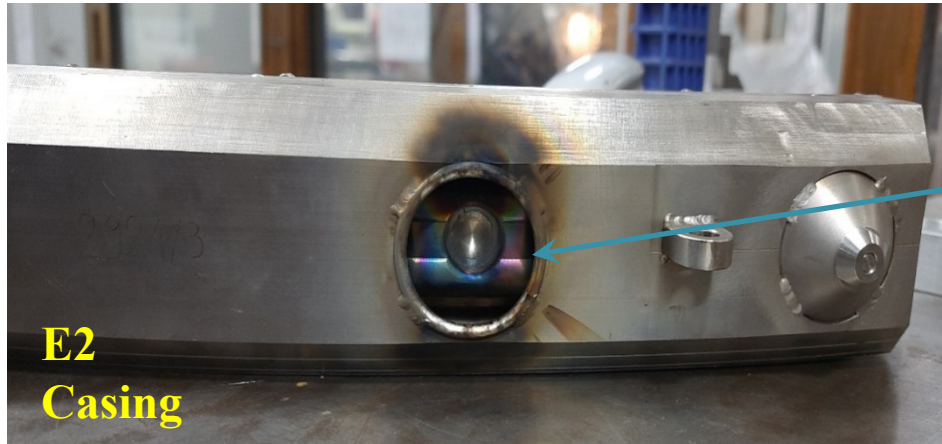
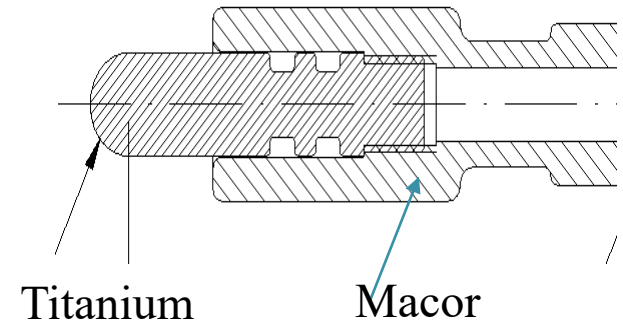
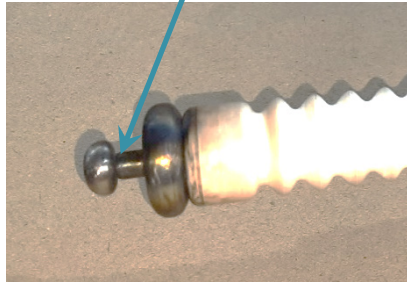
- ❑ Accelerated and extracted N^{2+} beam at 14 MHz RF,
- ❑ $h = 2$, Energy = 4.5 MeV/A
- ❑ Beam has been transported to Target in CAVE-1

- ❑ Accelerated N^{4+} beam at 14 MHz RF,
- ❑ $h = 1$, Energy = 18 MeV/A

INITIAL BREAKDOWNS DURING DEFLECTOR CONDITIONING

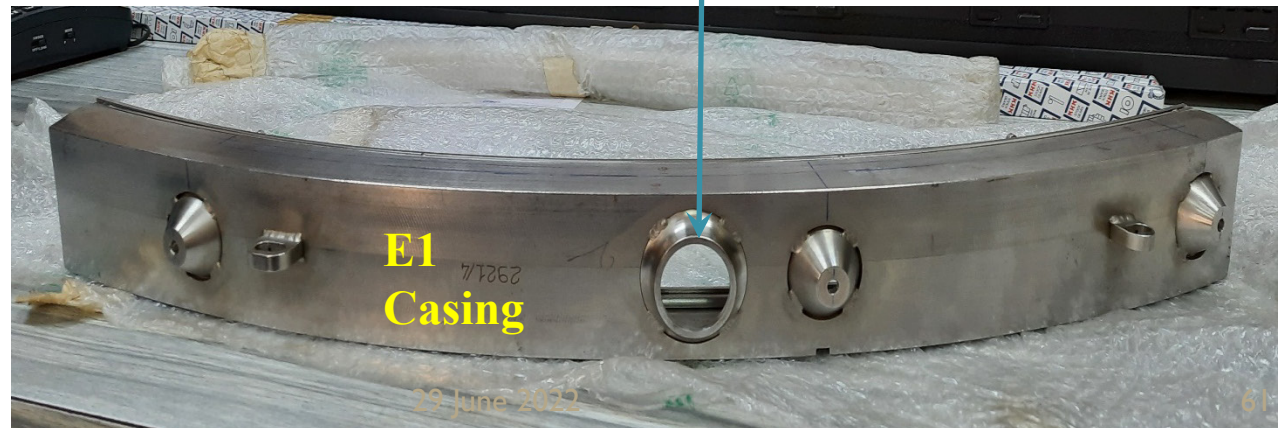


Modifying
this part



**E2
Casing**

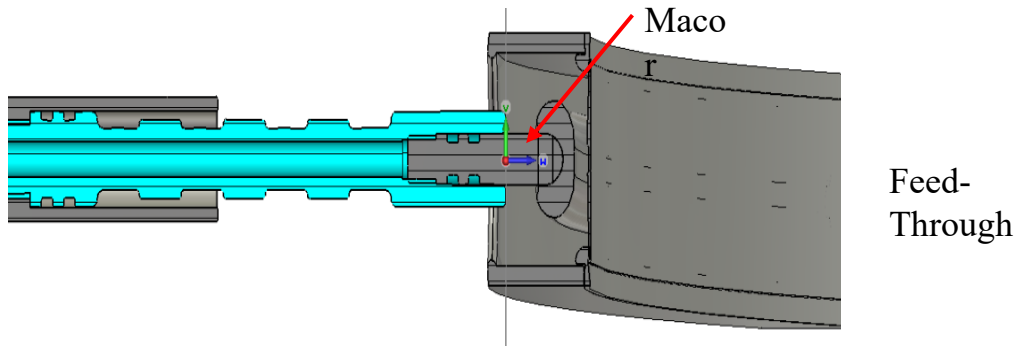
**Increasing the feed-
through Hole diameter
from 32 mm To 50 mm**



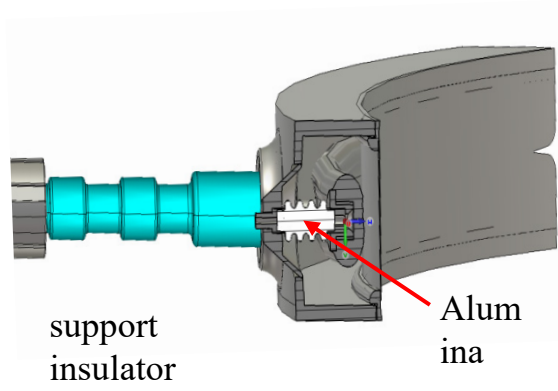
**E1
Casing**

TRYING TO ACHIEVE 80 KV IN 6 MM GAP ~ 14 KV/MM

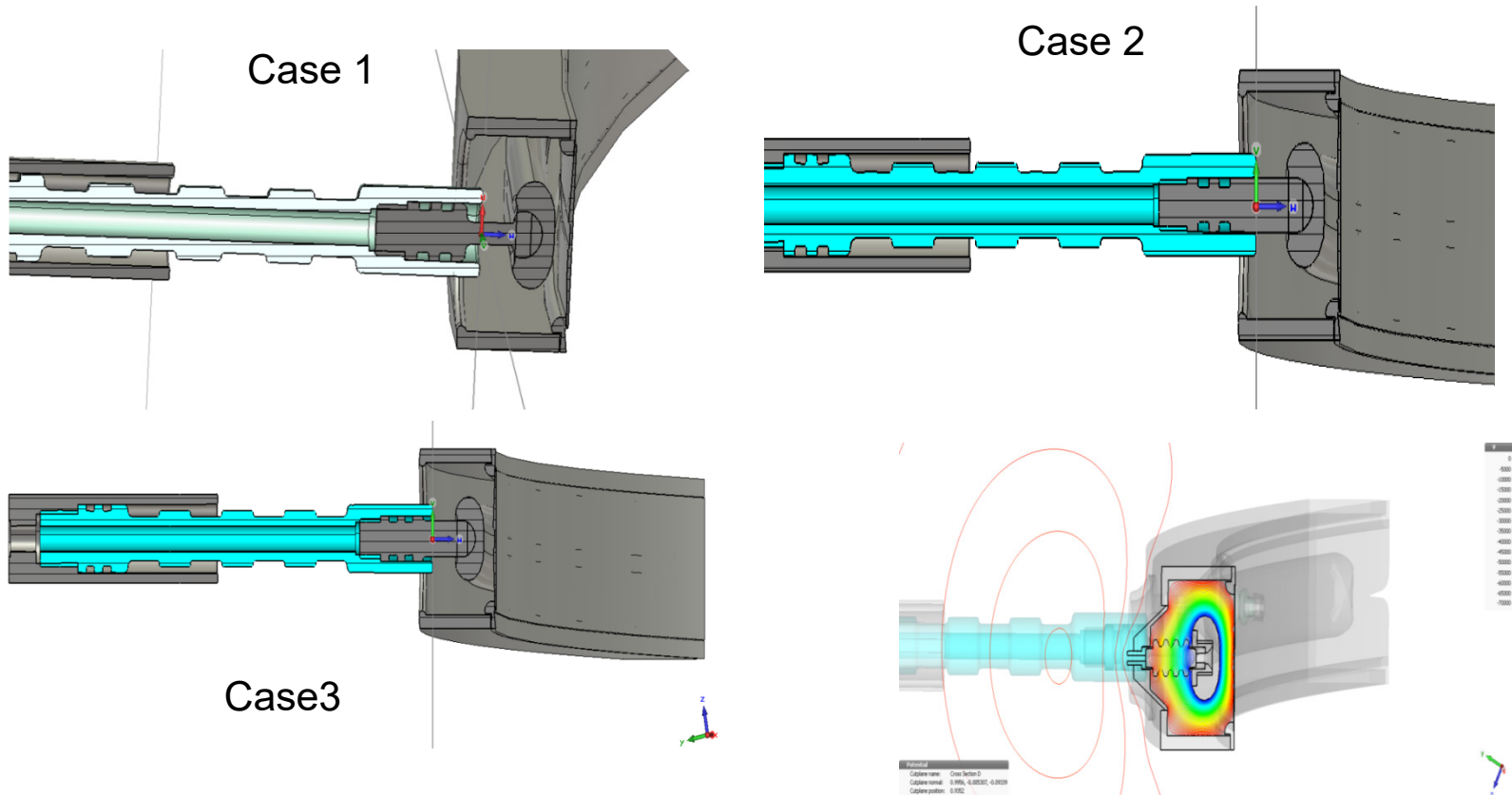
Pressure = 10^{-7} mbar



| Breakdown Voltage (kV/m) | |
|--------------------------|----|
| Air | 3 |
| High Vacuum | 20 |
| MACOR ^T | 40 |
| Alumina | 13 |



DEFLECTOR NEW FEED-THROUGH DESIGN STUDY AND MODIFICATION



Existing configuration: Support insulator ceramic
Proposed insulator MACOR

Ceramic, 96% Al_2O_3 ,
 Dielectric Constant ~ 7.8

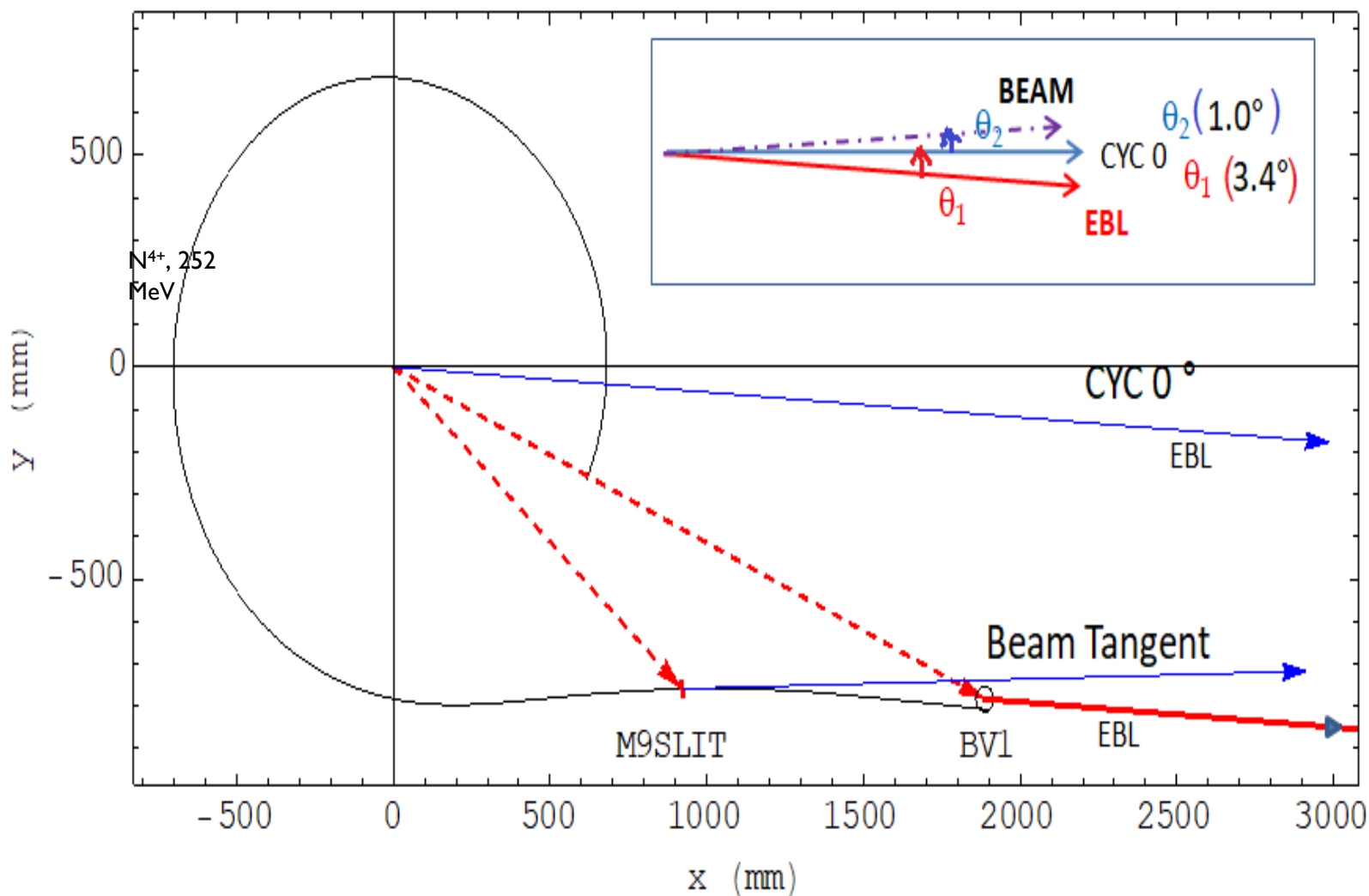
| Machinable Glass Ceramic (MACOR) | | |
|----------------------------------|--------------|--------------|
| $R_i=8.1$ mm | $R_i=6.5$ mm | $R_i=8.1$ mm |
| $R_o=12$ mm | $R_o=12$ mm | $R_o=12$ mm |

MACOR: 46% SiO_2 , 17% MgO , 16% Al_2O_3 , 10% K_2O , 7% B_2O_3 , 4% F
 Dielectric constant: ~ 6
 Thermal conductivity: $1.46 W/m^2K$
 Density: $2500 kg/m^3$

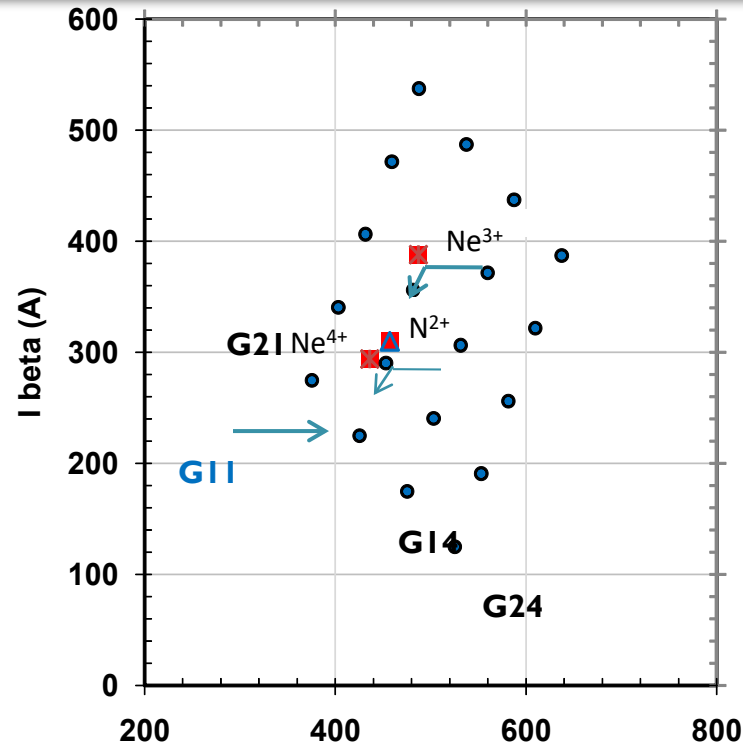
Extraction of N^{4+} beam (252 MeV) & Ne^{6+} (363 MeV)

- ❑ **After deflector conditioning up to 45 kV, beam run started for N^{4+} beam (252 MeV) at 14 MHz.**
- ❑ **N^{4+} beam has been extracted from the machine**
- ❑ **20 nA beam in FC01 and transported 4 nA beam in FC06 before the target**
- ❑ **Then Ne^{6+} beam (363 MeV) extracted from the machine**

EXTRACTED BEAM TRAJECTORY



MFM GRID POINTS :- PROBABLE ION BEAMS



Probable Ion beams

| ION | Q | A | Q/A | V_{RF} (MHz) | h | B (kG) | E (MeV/A) |
|-----|----|---------|--------|----------------|---|--------|-----------|
| Ne | 5 | 20.1797 | 0.2478 | 12.0 | 1 | 31.54 | 13.2 |
| Ne | 6 | 20.1797 | 0.2973 | 15.2 | 1 | 33.29 | 21.2 |
| Ne | 6 | 20.1797 | 0.2973 | 17.3 | 1 | 37.89 | 27.5 |
| N | 5 | 14.0067 | 0.357 | 20.2 | 1 | 36.87 | 37.5 |
| N | 4 | 14.0067 | 0.2856 | 17.0 | 1 | 38.77 | 26.5 |
| O | 4 | 15.9994 | 0.25 | 12.2 | 1 | 31.78 | 13.7 |
| O | 4 | 15.9994 | 0.25 | 14.6 | 1 | 38.03 | 19.6 |
| Ar | 12 | 39.9480 | 0.3004 | 14.0 | 1 | 30.35 | 18.0 |
| Ar | 12 | 39.9480 | 0.3004 | 17.6 | 1 | 38.16 | 28.4 |



Thank you

